N91-21198

PROPULSION SIMULATOR for MAGNETICALLY-SUSPENDED WIND TUNNEL MODELS

Prakash B. Joshi, C.L. Goldey, G.P. Sacco

Physical Sciences Inc.

20 New England Business Center

Andover

MA 01810

Pierce L. Lawing

NASA Langley Research Center

Mail Stop 238

NASA Langley Research Center

Hampton

VA 23665-5225

PROPULSION SIMULATOR FOR MAGNETICALLY-SUSPENDED WIND TUNNEL MODELS

P.B. Joshi, C.L. Goldey, and G.P. Sacco
Physical Sciences Inc.
Andover, Massachusetts

and

P. Lawing
NASA Langley Research Center
Hampton, Virginia

I. Introduction

The wind tunnel has been an indispensable tool for aeronautical research and aircraft configuration development for the past 80 years. During that period, tunnels have evolved in speed, increased in size, improved in flow quality, advanced in flow measurement techniques, and become sophisticated in the use of digital computers for data acquisition, reduction, and analysis. Throughout this advancement, the ability of the wind tunnel to faithfully simulate the aerodynamic forces and moments on a model, which can be related to the forces and moments on the full scale aircraft, has always been limited by uncertainties in measurements due to support and wall interference effects. Support interference can lead to significant errors in measured aerodynamic force and moment coefficients and static stability derivatives. These errors become very large at transonic speeds and/or high angles-of-attack. Magnetic suspension and balance systems (MSBS) were developed originally to eliminate the support interference problems. They also have the additional advantages of providing dynamic stability derivatives, two-body force measurements, and improved tunnel productivity. About 25 years ago wind tunnel development shifted emphasis from MSBSs to cryogenic tunnels which can duplicate the full-sale flight Mach and Reynolds numbers simultaneously. This capability has recently become available with the completion of the National Transonic Facility at NASA Langley Research Center (LaRC). Now, the community of experimentalists is advocating the development of MSBSs for large wind tunnels including the cryogenic tunnels. Further impetus for this development has been provided by advancements in the technologies of superconductivity, control systems, and computers.

One of the capabilities desired in magnetic suspension wind tunnels is the simulation of propulsison-induced aerodynamic forces and moments, which arise as a result of interactions beetween propulsive jets and the free stream. Such a simulation has always been a difficult task, even in conventional wind tunnels. The main reasons have been the problems of introducing high pressure air into the model, questions regarding proper scaling parameters, construction of models out of metric and non-metric sections, and accurately determining the force/moment contribution to the non-metric section. The model support is sometimes an advantage in that it provides a means of bringing air on-board either through ducts which can be secured to the support or through a passage drilled in the support. At times, however, the support can be a disadvantage in that it can prevent the discharge of air at the desired location, as would be the case for a sting support.

Propulsion simulation for magnetically suspended model presents special practical problems because there can be no physical connection between a compressed air reservoir and the model. Thus, propulsive gases must be generated on-board the model and then exhausted at desired locations on the model, Figure 1. The problem involves defining proper thrust (mass flow rate and velocity) requirements for the propulsive jet(s) and accomplishing gas generation within the volume of the model. Propulsion simulation in its entirety, whether for conventional or magnetically-suspended models, involves both engine intake and exhaust jet flows. Only the latter is addressed in the work presented here. Our rationale is that the first step in simulation of propulsion should be to introduce the effects of the exhaust jet and that the complexities of allowing properly matched inlet flows should be deferred to later stages of development.

Under Phase I of an investigation sponsored by NASA LaRC, the feasibility of generating exhaust jets of appropriate characteristics on-board magnetically-suspended models was examined. Four concepts of remotely-operated propulsion simulators were considered. Three conceptual designs involving conventional technologies such as compressed gas cylinders, liquid monopropellants, and solid propellants were developed. The fourth concept, a laser-assisted thruster, which can potentially simulate both inlet and exhaust flows, was found to require very high power levels (tens of kilowatts). This concept needs further research. The results of Phase I investigation, including a comparative evaluation of the four concepts, are discussed in Ref. 1.

The objective of current Phase II investigation sponsored by NASA LaRC is to demonstrate the measurement of aerodynamic forces/moments, including the effects of exhaust jets, in MSBS wind tunnels. Two propulsion simulator models are being developed, a small-scale and a large-scale unit, both employing compressed, liquified carbon dioxide as propellant. The small-scale unit has been designed, fabricated, and statically-tested at Physical Sciences Inc. (PSI). It will be tested, either as a part of a wind tunnel model or by itself, in the 7-in. University of Southampton MSBS tunnel to measure forces/moments with jet on/off. The MSBS hardware and software is presently being modified for this purpose to be compatible with the impulsive thrust forces associated with propulsive jets. The large-scale simulator is in the preliminary design stage as of this writing. It will be fabricated and statically-tested at PSI.

This paper presents the small-scale simulator design/development and discusses the data from its static testing on a thrust stand. The analysis of this data provides important information for the design of the large-scale unit. The paper concludes with a description of the preliminary design of that device.

II. Propulsion Simulator Design Considerations

Before describing the small-scale simulator, it is appropriate to discuss the design requirements. Since the existing MSBS wind tunnels [2] allow the installation of relatively small models, a very limited volume is available for a propulsion device. Further, the magnetic core used for levitation also needs some space within the model, and the restrictions on the size of the propulsion simulator can indeed be significant. The largest operational MSBS wind tunnel in the U.S. at NASA LaRC has a 13-in. diameter test section. Another MSBS facility at University of Southampton, England, which is more versatile in that it has angle-of-attack variation capability, has only a 7-in. wide test section. In this wind tunnel, the model envelope would typically be 6 to 8-in. in length with 1 to 1.5-in. diameter centerbody. In the NASA tunnel, models 18-in. long by 3-in. diameter can be installed.

Since no external connections can be made to bring jet fluid to a model in an MSBS, the propellant must be carried on-board. The model volume limitations directly translate into the mass of the propellant which can be stored on-board. In turn, this limits the duration over which the exhaust jet can be maintained. For practical applications, this means frequent model refurbishing and thus potentially reduced tunnel productivity with propulsion simulation.

Because no physical connections exist with a magnetically-levitated model, it is necessary to control the propulsive model remotely. Therefore, the source of electrical energy required to open/close valves or initiate ignition must either be carried on-board and triggered externally by such means as radio control or laser.

The characteristics of a particular MSBS also impose some restrictions on the propulsion simulator. These are the weight of the simulator module which can be suspended and the level of the thrust force. The restrictions arise due to the limitations on the amount of current which can be driven through the coils of the external electromagnets (Figure 1). Another consideration is that the model position changes due to the thrust rise (or fall) with time, when propulsion is turned on (or off). This movement must be controllable by the control system of the MSBS.

Finally, any propulsive gas generation technique must be compatible with the particular wind tunnel hardware involved and its operational requirements. Even small quantities of particulate matter or water vapor in the exhaust may not be acceptable in some facilities.s Furthermore, there may be considerations of safety of personnel, requiring special precautions in some cases.

The design considerations are summarized in Table 1. The implementation of these requirements into the simulator design is discussed in Ref. 1.

Perhaps the simplest propulsion simulator is a compressed gas cylinder attached to a nozzle and turned on/off by means of a remotely-controlled valve. However, the mass of gas which can be carried under reasonable pressures in volumes typical of a MSBS wind tunnel models, is so small that the resulting thrust time (or run time) will be of the order of tens of milliseconds. Furthermore, the gas container will have to be refilled under high pressure innumerable times, which makes this approach impractical. A way around this problem is to use gases that liquify easily under pressure at room temperature, so that a significantly larger mass can be stored in a given volume. Among common substances, the candidates are carbon dioxide (CO_2) and ammonia (NH_3). Table 2 lists the physical properties of these gases along with another substance, sulfur dioxide (SO_2) which has some desirable properties.

The ideal propellant gas should have a high density in liquid phase to pack as large a mass as possible in a given volume and a low molecular weight (see Appendix A). Low heat of vaporization is desired so that, as the liquid changes into vapor, it does not draw such a large amount of heat from itself and surrounding walls that it freezes. Low vapor pressure is also desirable, because it means that liquification occurs at lower pressure at a given temperature. Thus, the pressure regulation necessary to drop the pressure to say 45 to 60 psia (P_{0j}/p_∞ = 3-4) is relatively straightforward. That is, compact regulators, necessary in the present application, are easy to find.

Table 1. General Design Considerations for Propulsion Simulators

• Compactness	Smallest size possible for demonstration in current available MSBS tunnels
• High Density Propellant	Ability to carry the largest propellant mass in a given volume inside the model to maximize run time for a specified mass flow rate
• Relatively Lightweight	To minimize the size of magnetic core within the model and currents in external electromagnets
• Remote or Minimum Interference Activation	If remote activation is not feasible, the disturbance to flow field and magnetic field must be negligibly small
• Thrust Level	Compatible with particular MSBS capability
• Thrust versus Time Characteristics	Compatible with MSBS control system capability. Stable thrust duration must be sufficiently long so that data can be obtained after model becomes steady
• Safe Operation	Propellant material should be non-toxic, non-corrosive, with minimum of particulates

Table 2. Physical Properties of Propellant Gases

Gas	Molecular Weight	Vapor Pressure at 70°F (psi)	Density of Liquid (gm/cm^3)	Heat of Vaporization (cal/gm)
CO_2	44	840	0.75	36
NH_3	17	129	0.61	283
SO_2	64	50	1.38	83

An examination of Table 2 shows that each gas has certain advantages and disadvantages. Ammonia has the lowest molecular weight and reasonably low vapor pressure, but it has extremely high heat of vaporization and the lowest density. Sulfur dioxide, on the other hand, has the lowest vapor pressure and highest density (38 percent above water), but the latter is offset by its high molecular weight. The heat of vaporization of SO_2 is considerably lower than that of NH_3. Carbon dioxide has a molecular weight between that of NH_3 and SO_2, the lowest heat of vaporization, and density slightly higher than that of ammonia. A disadvantage of CO_2 is its high vapor pressure (56 atm).

There are some practical advantages of CO_2 that make its choice as a propellant almost inevitable. It is commercially available in cartridges (or cylinders) which vary in weight from a few grams to hundreds of grams. The cylinders are very compact, a cylinder containing 16g of CO_2 measures 3.5 in. long × 1.6 in. diameter, a 60g cylinder measures 5.1 in. long × 0.865 in. diameter.

As these cylinders have wide commercial applications (air guns, life vests, inflatable boats, beverage industry), they are available in any desired quantity at a very low cost. For example, the price of a 16g CO_2 cylinder is less than $2. Another advantage of these cylinders is that they are available in stainless steel (which is non-magnetic) or as magnetizable steel. This is potentially useful because the mass of the cylinder itself can serve as a part o the magnetic core. CO_2 cylinders can be obtained as customized components from Sparklet Devices, Inc.

CO_2 also has some operational advantages over NH_3 and SO_2. In practice, the mass flow rate of the gases will be small (< 100 g/s) compared to that in the wind tunnel (~2 kg/s in University of Southampton 7-in. tunnel and 7 kg/s in NASA LaRC 13-in. tunnel) and the duration will be typically less than 5s for one thrusted run. Thus the propellant gases will get quickly mixed, diluted, and dispersed int he wind tunnel-free stream. In open circuit tunnels, of course, the products will leave the test section and not be circulated. CO_2 is a clean, non-contaminating, non-corrosive, and safe gas. NH_3 and SO_2 on the other hand are somewhat corrosive, and can be irritants to eyes and lungs, if released accidentally. The use of these gases then entails special precautions not necessary to CO_2.

Some disadvantages of the compressed gas concept are that miniaturized, remotely operated valves are required to turn the jet on/off, and further, a battery power supply and switch must be incorporated in the model. An inherent limitation of the concept is that the total temperature of the jet is close to room temperature. Therefore, a hot jet is not possible unless heat is added before exhausting the gas, which represents an additional complication. The problem of cooling of the cylinder as the liquid vaporizes can be minimized by surrounding the cylinder with an annular magnetic core which can provide the necessary thermal mass.

It is shown in Appendix A that the thrust and mass flow ranges for a propulsive jet on a typical 1/40-scale model of a fighter aircraft are 2.5 to 3.2 kgf and 0.08 to 0.01 kg/s of CO_2 gas, respectively.

The primary objective of the present work is to demonstrate the operation of a thrusting, propulsive model in an MSBS, and to measure the resulting forces/moments. The University of Southampton wind tunnel to be used for testing has a 7-in. octagonal test section. The small test section size and the desire to achieve high angles of attack (~45 deg), limits the model size. This limitation, in turn, restricts the number and the size of flow control components (a pressure regulator, an on/off solenoid valve, for example) that can be incorporated into the model. It was decided, therefore, to design and build two models: a small-scale simulator for demonstration in an MSBS and a large-scale simulator for static testing only. The small-scale model was developed principally to (1) demonstrate generation of an exhaust jet using CO_2 propellant, (2) guide in the design of the large-scale unit, and (3) verify the control and force/moment measurement of a thrusted model in the Southampton MSBS. The larger model, currently in preliminary design stage, is being developed to (1) generate exhaust jets of desired characteristics, and (2) demonstrate the feasibility of propulsion simulation on larger wind tunnel models representative of practical applications.

The large-scale simulator will be a versatile design for generating a jet with pressure ratio, mass flow, and thrust requirements outlined in Appendix A. Furthermore, this design will permit intermittent, on/off operation of the jet. By contrast, the small-scale simulator is designed to be such that the propellant and some components must be replaced after every jet "run". Moreover,

no attempt is made to tailor the jet characteristics to the requirements of Appendix A for the small-scale device.

III. Small-Scale Propulsion Simulator Design

Figure 2 shows the small-scale simulator design which is a 1-1/8-in. diameter cylinder, 8-in. long, with hemispherical ends. The principal components are a 16g, liquified CO_2 cylinder (manufactured by Sparklet Devices), a cap-piercing hardened pin and squib mechanism (adapted from a design by Special Devices, Inc. (SDI)), battery and electronics assembly housed in the nose, three removable sets of copper spheres, and a nozzle. These components are housed inside a tube, 1/8-in. thick, made from an electromagnetic alloy formulated by Connecticut Metals, Inc. (CMI). The total weight of the simulator is about 600g with approximately 500g of magnetizable materials. The latter includes the material of the CO_2 cylinder and other miscellaneous components such as retainer rings, fasteners, spacers, etc. Figure 3 shows the distribution of the magnetizable mass in the simulator.

The simulator consists of three major subassemblies: nose section, center section, and nozzle section. The nose section, which screws onto the center section, contains the battery (Kodak K28A) used as a power source for firing the squib (made by Cartridge Actuated Devices, Inc.) and the electronics assembly. The latter consists of a light-activated switch (EG&G, VTIC1110), a small mirror, and a silicon controlled rectifier, all mounted on a 0.06-in. thick circuit board. The battery is held inside a retaining clamp onto which the circuit board is mounted. An optical filter is embedded in the wall of the nos section. The filter allows HeNe laser wavelength (632.8 nm) to pass to the light activated switch. A pair of 22 AWG wires runs from the circuit board to the squib in the center section.

The center section of the simulator contains the CO_2 cartridge with its threaded neck screwed into a cylinder retainer which is held in place by a squib retainer. The pin-squib mechanism (made by SDI) is screwed into the threaded hole at the center of the squib retainer. The SDI design was modified such that inexpensive squibs made by Cartridge Actuated Devices could be incorporated into it. Had this modification not been done, the complete SDI pin/squib mechanism would have required replacement after each firing, costing about $150. Our design modification makes it possible to replace the squib only, for approximately $5 to $10. Earlier in the program, the "standard" piercing pin in the SDI component was used. This pin (also called "large" pin) as shown in Figure 4(a), had an internal hollow passage 0.050-in. diameter to draw CO_2 from the cylinder. Two holes, 0.050-in. diameter, in the 0.045-in. thick walls of the standard pin, expel the CO_2 into a stagnation chamber. The gas then flows from the chamber into a cavity surrounding the squib assembly through four oval passages drilled into the squib retainer (Figure 5). Another pin, with smaller outside and inside diameters, and with smaller ports for expelling CO_2, was also used during development, Figure 4b. Both pins were case-hardened to ensure reliable penetration of the diaphragm of the CO_2 cylinder. Moreover, hardening also improved the usable life of the firing pin. Two holes (not shown in Figure 2) are drilled into the wall of the center section for measuring pressure in the stagnation chamber and in the cavity upstream of the nozzle section. The two 22 AWG wires connecting the squib to the electronics in the nose section pass through a lengthwise groove machined in the wall of the center section.

The nozzle section screws onto the backend of the center section of the simulator. It contains three baffle assemblies which can be loaded with copper spheres of 1 or 2 mm diameter.

Each assembly consists of a copper housing (a ring as shown in Figure 2) with a copper wire mesh at each end for retaining the spheres. Each assembly can be individually removed and replaced by a ring made of the CMI electromagnetic alloy. The purpose of the three copper plugs was to introduce a drop in total pressure as the CO_2 negotiated a tortuous path, and secondly, to vaporize any fine solid particles of CO_2 which may be present in the flow. As will be discussed later, the copper plugs were not always effective. A convergent passage was drilled into the nozzle with a baseline diameter of 0.098 in. A separate nozzle section with exit diameters of 0.298 in. was also used. Both nozzle sections were tested. The larger nozzle, used on a 1/40-scale model, corresponds to 12-in. full-scale throat diameter. A pressure tap was drilled into the nozzle wall downstream of the copper plugs and upstream of the exit orifice.

The operation of the small-scale simulator consists of shining a HeNe laser beam onto the optical filter in the nose section. The light switch is activated and the SCR then draws approximately 1 amp current from the battery to fire the squib. Explosion of the squib drives the pin (which moves against O-ring friction) into the diaphragm which caps the CO_2 cylinder. Only about 45 psi pressure is needed to rupture the diaphragm and the squib supplies 70 to 150 psi from the gaseous products of explosion. After penetration the pin stays in place due to the friction of the O-ring inside the housing of the SDI squib assembly. CO_2 liquid-gas mixture flows through the center passage in the pin and escapes through the two holes drilled in the walls (Figure 4). Upon passage through the squib retainer (Figure 5), the CO_2 flows through the copper plug(s) into the nozzle chamber and out through the orifice producing a jet.

IV. Results of Static Testing of Small-Scale Simulator

As mentioned under Design Considerations, the small scale model was developed primarily to verify the control of and force/moment measurement on an impulsively-thrusted model in an MSBS and to guide in the design of the large-scale unit. Toward these objectives, a series of static tests was conducted. The tests were designed to yield thrust versus time history and pressure versus time history, the latter at three locations within the simulator. The thrust versus time data are necessary for design of the MSBS control system so that the model stays in place as it reacts to the propulsive jet turning on/off. The pressure data, which are diagnostic in nature, provide important insight into the effectiveness of the copper plug(s) in creating a pressure drop and into the gas dynamic processes within the simulator.

The schematic of the static-test set-up is shown in Figure 6. A load cell manufactured by Sensotec was used to obtain force (i.e., thrust) data. The pressure transducers were supplied by D.J. Industries and located as shown in Figure 6b. The pressure P_2 and P_1 give a measure of the effectiveness of the copper spheres in creating a pressure drop. The pressures P_2 and P_3 give a measure of the gas dynamic processes and losses due to jet impingement on the cylindrical walls of the simulator. The load cell and transducer signals were sampled at 1 kHz. Visual observations of the jet just outside the nozzle exit plane indicated whether or not mist was present. The presence of mist shows that the copper spheres were not very effective in vaporizing the tiny solid particles formed during the expansion of CO_2 from compressed liquid to vapor.

The test variables were:

- Simulator orientation:

  In the vertically-up orientation shown in Figure 6a, vapor rather than liquid is being drawn through the pin upon its penetration into the CO_2 cylinder. In a vertically-down configuration, one expects the liquid to be drawn through the pin, and the vaporization to take place in the stagnation chamber (pressure P_3 in Figure 6a). Of course, in practice, the simulator will be used mostly in a horizontal position or with the jet pointing downward, except in few instances of negative angle-of-attack. The effects of simulator orientation, therefore, are expected to be important. Static tests were conducted in all three orientations.

- Copper plug structure:

  The copper plug(s) were introduced in the small-scale simulator to act as a pressure-drop device and also to aid in vaporizing small solid particles in the CO_2 stream. The data on effectiveness of the plug in performing these functions are necessary to guide the design of the large-scale simulator. For example, a pressure regulator and a heater (i.e., vaporizer) may have to be incorporated, if the copper plugs are found to be not very effective.

- Pin design:

  The internal passage diameter of the piercing pin (Figure 4) determines the maximum possible mass flow rate through the propulsive device and thus its internal pressure and thrust versus time characteristics. Tests were conducted using a so-called "standard" or "large" pin, Figure 4a, and a "small" pin, Figure 4b.

- Nozzle diameter:

  The nozzle diameter determines the actual mass flow rate through the simulator and thus thrust level duration. Further, the nozzle area is an important design parameter of the aircraft configuration being tested. Two values of diameter, 0.098 and 0.295, were used in the static tests.

Selected data from the simulator tests are presented in Figures 7 through 16. Each figure contains thrust and pressure versus time history. The three pressures, P_1, P_2, and P_3 are given on the same plot. Appendix B contains the small-scale simulator test matrix.

Figure 7 shows thrust and pressure curves for the baseline simulator configuration without any copper plugs. After an initial spike which reaches 4 lbf, the thrust rises to a maximum of about 1.9 lbf in about 0.1s and decreases gradually over the next 1.2s. An average thrust of about 1 lbf over a duration of 0.5s is achieved. The rise in thrust is due to the increase of pressure as the CO_2 fills up the simulator volume. The fall in thrust thereafter is directly due to the dropping stagnation pressure inside the simulator as the CO_2 escapes through the nozzle. The thrust behavior correlates well with the pressure history in Figure 7b. The pressures P_2 and P_3 are

coincident in this figure. Unfortunately, the P_1 transducer was overpressurized and saturated during this run. The initial spike in Figure 7a is a ubiquitous feature of most thrust data. It represents the impact of the piercing pin on the diaphragm of the CO_2 cylinder. The duration of this spike is a few milliseconds. It should also be pointed out the time elapsed from the instant that the laser triggers the light-activated switch to the instant the pin impacts the cylinder is of the order of 20 to 50 ms. This interval includes the electronics reaction time and the firing of the squib.

Figure 8 shows thrust and pressure histories when three sets of copper plugs, each packed with 2 mm diameter copper spheres, are placed upstream of the nozzle. A comparison of Figures 7 and 8 shows that the thrust curves are nearly the same and the pressures are also substantially similar. Thus, for the simulator with a large (or standard) piercing pin, the copper plug has little effect on the flow and pressures inside the simulator.

Figures 9 and 10 show the effect of simulator orientation on thrust and pressure characteristics. In Figure 9, the simulator was horizontal and incorporated the same copper plugs as the configuration in Figure 8. The peak thrust in the horizontal orientation is slightly higher and falls off somewhat faster than the vertically-up orientation of Figure 8. The data in Figure 9 is also more noisy and is believed to be an artifact of the simulator cantilevered from the load cell. The pressures in Figure 9b are seen to be greater than those in Figure 8b, which explains the thrust behavior. Figure 10 shows data for the simulator firing the jet vertically down. The copper plugs are the same as for Figures 8 and 9. A comparison between Figure 8 and Figure 10 reveals that the thrust is substantially higher when liquid CO_2 is drawn because greater mass of CO_2 enters the stagnation chamber in a given time. Further, the thrust maintains its higher level for about 0.5s before beginning to drop-off rapidly. This behavior suggests that the liquid CO_2 escaping into the stagnation chamber of the simulator (Figure 2) vaporizes. During this process, liquid-vapor equilibrium is maintained, and the pressure tends to remain constant. However, the pressure drops as the CO_2 vapor leaves through the nozzle. The net effect of these two opposing processes is to reduce the rate at which pressure and thrust drop. A comparison of Figures 10b and 8b shows higher pressure for the vertically-down orientation. Also, the behavior of pressure with respect to time in Figure 10b explains the thrust history in Figure 10a.

Figure 11 shows an interesting observation when the CO_2 mass flow rate into the stagnation chamber is extremely high. This condition occurred when the piercing pin was pushed back (due to the wear of an O-ring in the squib assembly) by the high pressure CO_2, resulting in efflux through a larger area (0.095-in. diameter) than the normal two-hole configuration (0.05-in. diameter each), Figure 4. The consequence is very high peak thrust, ~5 lbf which drops off rapidly, Figure 11a. The pressure has now reached a very high value, almost 600 psi, Figure 11b.

Figure 12 illustrates the effect of changing the copper plug arrangement to one set of 1 mm diameter copper spheres and tightly packed bronze wool replacing the other two sets. Comparison with Figure 8 shows the thrust and pressure histories to be very similar in both cases. Thus, the structure of the plug has very little effect on the flow processes within the simulator. Note in Figure 12b that the three pressures, P_1, P_2, and P_3 at different locations (Figure 6) are very close. This indicates that with the 0.098-in. diameter exit nozzle, the simulator behaves essentially like a closed vessel which is pressurized by the CO_2, maintaining pressure equilibrium throughout its volume. This would explain the ineffectiveness of the copper plug observed thus far.

Figure 13 shows the effect of reducing the mass flow rate from the CO_2 cylinder by using the "small" pin design of Figure 4b. Comparison with Figure 12, which presents data for the large pin in Figure 4a, reveals lower thrust level and longer duration with the small pin, as one would expect. The peak thrust is approximately 1.4 lbf and the average thrust is about 0.75 lbf over 0.75s. The pressures with the small pin (Figure 13b) are correspondingly lower in comparison with the large pin (Figure 12b).

Figure 14 through 16 contain data of the case of a larger nozzle diameter (0.295 in.) with both the large and small piercing pins. With the standard, large pin, the thrust in Figure 14a may be compared with Figure 12a. As one would expect, with a larger nozzle, the pressures are lower (Figures 14b versus 12b) and the thrust is lower, but it drops off at a slower rate. The slower rate is due to reduced mass flow rate through the nozzle, resulting from lower (i.e., subsonic) pressure ratio relative to the ambient. The effect of removing the copper plug with the 0.295-in. diameter nozzle on the simulator is to decrease significantly the thrust as seen from Figure 15a, indicating that the plug, rather than the nozzle, was the controlling area for the mass flow rate. The pressures throughout the simulator volume, especially upstream of the nozzle, are low (and noisy), Figure 15b. Finally, Figure 16 illustrates the thrust and pressure histories for the simulator configuration with a 0.295-in. diameter nozzle, "small" pin, and a plug made of one set of 1 mm diameter copper spheres plus bronze wool. When compared with "large" pin data of Figure 14, the thrust (and pressures) are lower with the small pin.

During the series of static tests, visual observations of the CO_2 jet from the nozzle indicated presence of white mist frequently, even with the copper plugs and bronze wool in place. Thus the effectiveness of the copper spheres in vaporizing solid particles upon contact is questionable. It is possible that the particles are so fine that they follow the gas streamlines without actually making contact with the spheres.

It can be summarized from results of the static tests of the small-scale simulator that a working device for wind tunnel testing in the University of Southampton's MSBS has been developed. Toward the design of the large-scale simulator, it appears that the copper plugs have little effect on pressure regulation (especially at the higher mass flow rates and higher thrust level with the small diameter nozzle) and on solid particle vaporization. The internal passage diameter of the piercing pin which controls the mass flow rate from the CO_2 cylinder has a significant effect on the simulator's thrust and fluid dynamics. Finally, as expected, the spatial orientation of the simulator has a significant effect on its thrust characteristics.

V. Large Scale Propulsion Simulator Preliminary Design

As mentioned earlier, the large-scale simulator design is based upon the lessons learned from the small-scale simulator experience. The large-scale device is intended only for static testing on a thrust stand. It is apparent from the review of the small-scale test data that an active pressure control component and a means of vaporizing small solid CO_2 particles must be incorporated into the large-scale design. Furthermore, one must be able to turn the simulator on/off during wind tunnel testing. The thrust and mass flow requirements are as defined in Appendix A.

Taking the above requirements into account, a preliminary design of the large-scale simulator, shown in Figure 17, has been developed. The overall envelope is 2.5-in. diameter and

16-in. long. It incorporates an aluminum cylinder made by Clift Impact Division of Parker Corporation for CO_2 storage. The cylinder incorporates a siphon to ensure that liquid CO_2, rather than vapor, is drawn to meet the large mass flows required (~80 g/s). The flow of liquid CO_2 is turned on/off by a miniature solenoid valve made by General Valve Corporation. It is operated by an on-board battery via a light activated switch. The liquid CO_2 flows through numerous conduits drilled inside a heated copper block and vaporizes in the process. More heat is added to the CO_2 as it flows through a vaporizer which incorporates a number of thin, twisted plates to provide large surface area. The entire copper block/vaporizer assembly is wrapped in a 150W Kapton film heater and surrounded by insulation. The heater will be run on external AC power prior to a propulsion test run. In MSBS applications, the power connection can be in the tunnel walls or at the model itself. In the former case, it may be permissible to let two small wires float in the wind tunnel stream. The flow from the vaporizer enters a pressure regulator (Tescom Corporation) which can be set to yield the required pressure ratio across the nozzle. The regulator must maintain a constant outlet pressure as its inlet pressure varies from approximately 900 to 100 psia. For nozzle pressure ratios of 2 through 5, the nozzle pressure must in the range 30 to 75 psia. The flow from the regulator enters a nozzle chamber through a series of holes drilled into an impingement plate. The function of this plate is to distribute the flow uniformly. The entire simulator assembly will be contained in a cylinder machined out of the electromagnetic alloy developed by CMI Company. The estimated weight of the large scale simulator is 3.9 kg including 1.9 kg of magnetizable materials.

As of this writing, all the components for the large scale design have been selected and detail design is in progress.

VI. Summary of Results

A small-scale propulsion simulator has been developed and statically-tested to determine its thrust versus time characteristics. The device will be tested in the University of Southampton MSBS wind tunnel in the near future.

The mechanical and electronics systems of the small-scale simulator were thoroughly tested and improved as necessary during the static tests. Hardened piercing pins have been developed and O-ring (inside the squib assembly) replacement frequency has been established to substantially increase reliability of the device.

The copper plugs incorporated in the small-scale design appeared to have little effect on pressure regulation or on vaporization of small, solid CO_2 particles. Although not entirely conclusive, this points to the need of a pressure regulator and a vaporizer device in the large-scale simulator design.

Static tests of the small scale simulator have shown that its spatial orientation has a significant effect on the thrust versus time characteristics. Furthermore, the internal passage diameter of the piercing pin, which controls the mass flow rate from the CO_2 cylinder, has a significant effect on the simulator's thrust and fluid dynamics.

Based on the experience from the small scale simulator development and testing, a preliminary design of the large-scale simulator has been completed. Detail design of this device is in progress. This simulator will be subjected to static tests later in this program.

VII. Recommendations for Future Work

The large-sale simulator currently being developed needs further design trade-off studies. The pressure regulator and vaporizer components are compact, but still they take up substantial volume and weight which would otherwise be available for additional propellant. Although the use of porous media (copper spheres, bronze wool) has not proved effective in the small-scale simulator, it must be recognized that the volumes employed were modest (1-in. diameter × 1-in. long cylinder). Also, the influence of the flow area of the porous plug relative to nozzle area has not been fully investigated thus far. It is possible that a substantially longer porous plug (yet smaller in length than the regulator plus vaporizer) may be effective. To determine this, it will be useful to develop an analytical model of the flow within the simulator and of the vaporization/ efflux from the CO_2 cylinder. Such a model can be used for parametric design studies characteristics and for predicting thrust versus time behavior.

VIII. References

1. Joshi, P.B., et al., "Propulsion Simulation for Magnetically-Suspended Wind Tunnel Models," Physical Sciences Inc., PSI-2055/TR-859, NASA Contract No. NAS1-18616, September 1988.

2. Tuttle, M.H., Kilgore, R.A., and Boyden, R.P., "Magnetic Suspension and Balance Systems, A Selected, Annotated, Bibliography," NASA TM 84661, July 1983.

Acknowledgements

This work was supported by NASA Langley Research Center under Contract No. NAS1-18845. The authors wish to acknowledge the comments and contributions of Dr. Evan Pugh at Physical Sciences Inc. and Dr. Michael Goodyear at University of Southampton during this investigation.

APPENDIX A

Reference 1 shows that the characteristics of current jet engines require

$$\frac{\dot{m}}{A}\sqrt{RT_{oj}} \approx 1000 - 1200 \text{ lbm/in}^2\text{-s} \cdot \text{ft/s} \tag{A-1}$$

$$\frac{T}{A} \approx 40 - 50 \text{ lbf/in}^2 \tag{A-2}$$

$$\frac{P_{oj}}{p_\infty} \approx 2.5 - 4.5 \tag{A-3}$$

where:

$\dot{m}$	=	mass flow rate lbm/s
A	=	nozzle throat area
R	=	R_{univ}/mol wt
	=	gas constant of propellant, ft-lbf/lbm °R
T_{oj}	=	stagnation temperature of exhaust, °R
T	=	thrust, lbf
P_{oj}	=	stagnation pressure of exhaust, lbf/in^2
p_∞	=	ambient pressure, lbf/in^2.

To keep $\dot{m}$ small (for maximum "run" time out of a given storage volume), T_{oj} must be high and molecular weight low - i.e., higher jet velocity. The area A is determined by geometrical scaling of the model. The pressure ratio is determined by similarity of jet expansion characteristics.

It is of interest to determine the mass flow rates of typical propellant gases from the requirements stated above. For this purpose an exit area for the jet, A, must be chosen. The 1/40-scale throat area for an F-404 engine at maximum power is approximately 0.14 in.^{2} or 0.43-in. diameter. Table A-1 shows the required mass rates for typical gases, carbon dioxide and helium, at room temperature (300°K) and at 1200°K. It is clear that helium at high temperature has the smallest mass flow rate. However, in a typical 5s run, approximately 60g or 15 moles of helium will be needed. For this amount of helium to be carried in a cylinder approximately 1-in. diameter and 5-in. long, the required pressure will be in excess of 5000 atm or density greater than 1 gm/cm^3! As discussed in the main text, carbon dioxide is a more attractive propellant in spite of its greater molecular weight because it can be carried in liquified form under pressure.

Table A-1. Typical Mass Flow Rate and Thrust Requirements

Gas	Molecular Weight	Mass Flow Rate*, g/s		Thrust (kgf)
		@ T^o = 300°K	@ T^o = 1200°K	
CO_2	44	80-100	40-50	2.5-3.2
He	4	25-30	12-15	2.5-3.2
*A = 0.14 in.^{2} (0.43-in. diameter) with parameters as specified by Eqs. (A-1) to (A-3).				

The mass flow requirements in Table A-1 must be adjusted if a smaller jet area must be chosen due to model size constraints dictated by common MSBS wind tunnels. A 1/40-scale F-16 (which has the F-404 engine) has a wing span of 9.3 in. and can be accommodated in the 13-in. NASA LaRC MSBS tunnel, but not in the University of Southampton tunnel.

APPENDIX B

Small Scale Simulator Test Matrix

Test No.	Configuration			Pin Size	Comment
	Orientation	Cu Plug	Nozzle Diameter (in.)		
1	Vertical (up)	2 mm-1 set	0.098	Large	No pressure data
2	Vertical (up)	2 mm-1 set	0.098	Large	Cylinder didn't open - pin OD was larger than center section of bottle diaphragm
3	Vertical (up)	None	0.098	Large	Good
4	Vertical (up)	2 mm-1 set	0.098	Large	Dull pin
5	Vertical (up)	2 mm-1 set	0.098	Large	Repeat of 4
6	Vertical (up)	2 mm-1 set	0.098	Large	Hardened pin - OD too large
7	Vertical (up)	2 mm-1 set	0.098	Large	Pin OD turned down by 0.005 in. - worked
8	Vertical (up)	2 mm-3 sets	0.098	Large	Good shot
9	Vertical (up)	2 mm-3 sets	0.098	Large	Blocked pin orifice
10	Vertical (up)	2 mm-3 sets	0.098	Large	Pin pushed out of CO_2 cylinder, overpressurization, P_1 transducer failed
11	Vertical (up)	2 mm-3 sets	0.098	Large	Good shot, no P_1 data
12	Horizontal	2 mm-3 sets	0.098	Large	Good shot, not much CO_2 cloud
13	Horizontal	2 mm-3 sets	0.098	Large	Good shot, repeat of 12
14	Vertical (down)	2 mm-3 sets	0.098	Large	Good shot, repeat of 13
15	Vertical (down)	2 mm-3 sets	0.098	Large	Good shot, repeat of 14

Small Scale Simulator Test Matrix (Continued)

Test No.	Configuration			Pin Size	Comment
	Orientation	Cu Plug	Nozzle Diameter (in.)		
16	Horizontal	2 mm-1 set 1 mm-2 sets	0.098	Large	Pin pushed out of bottle, P_1 working
17	Horizontal	2 mm-1 set 1 mm-2 sets	0.098	Large	Good shot, redo 16
18	Horizontal	2 mm-1 set 1 mm-2 sets	0.098	Large	Good shot, repeat of 17
19	Horizontal	2 mm-1 set 1 mm-2 sets	0.098	Large	Good shot, repeat of 18. P3 adjusted to measure total pressure
20	Horizontal	1 mm-1 set bronze wool	0.098	Large	Good
21	Horizontal	1 mm-1 set bronze wool	0.098	Large	Good
22	Horizontal	1 mm-1 set bronze wool	0.098	Small	Pin pushed out of bottle - OD of pin same as large pin
23	Horizontal	1 mm-1 set bronze wool	0.098	Small	Redo 23 - good run. OD reduced. Note P_2vP_3 pressure drop, longer run at flatter thrust
24	Horizontal	1 mm-1 set bronze wool	0.098	Small	Repeat of 24
25	Horizontal	2 mm-1 set bronze wool	0.295	Large	Very high thrust, short run 0.2s, $P_2 \sim P_3$, P_1 low - substantial drop through plug
26	Horizontal	2 mm-1 set bronze wool	0.295	Large	Redo 25, good
27	Horizontal	2 mm-1 set bronze wool	0.295	Large	Repeat 26

Small Scale Simulator Test Matrix (Concluded)

Test No.	Configuration			Pin Size	Comment
	Orientation	Cu Plug	Nozzle Diameter (in.)		
28	Horizontal	None	0.295	Large	Initial "ringing" in thrust profile. Pressures too low, in transducer noise, 60 cycle noise on force
29	Horizontal	None	0.295	Large	Redo 28, same result
30	Horizontal	1 mm-1 set bronze wool	0.295	Small	Low thrust level, longer run
31	Horizontal	1 mm-1 set bronze wool	0.295	Small	Repeat of 30

Notes:

1. The P_1 pressure transducer saturated during Test 8 and failed during Test 10. It was replaced in Test 16.

2. Following Test 19, the orientation of the CO_2 jet from the pin was adjusted such that it impinged directly on the P_3 pressure port, providing a more reliable measure of stagnation pressure.

3. Pressure transducer ranges were:

   P_3: 1000 psi
   P_2: 500 psi for runs < Test 16
   : 5000 psi for runs ≥ Test 16
   P_1: 100 psi for runs < Test 16
   : 500 psi for runs ≥ Test 16

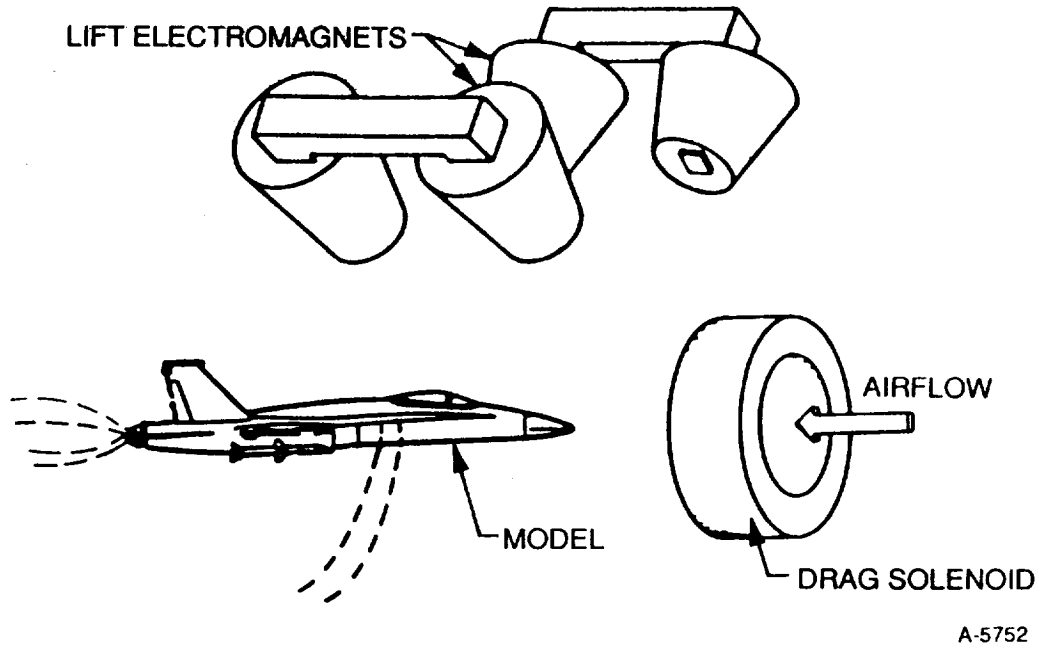

Figure 1. Schematic of Propulsion Simulation on a Magnetically Suspended Model

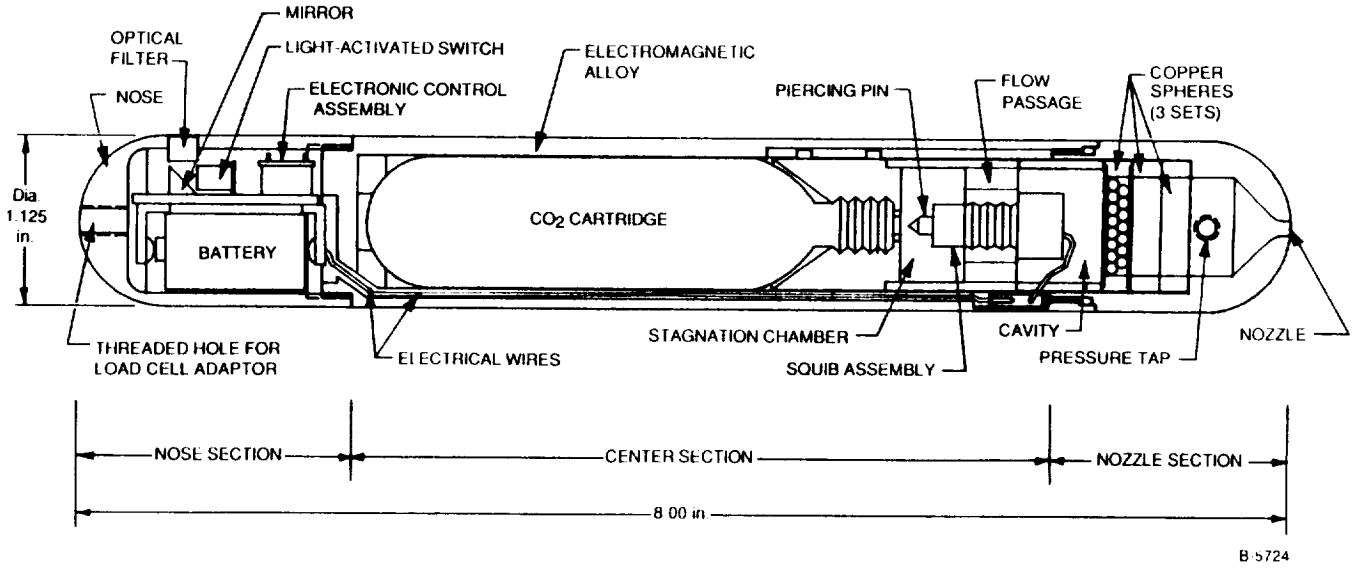

Figure 2. Small-Scale Propulsion Simulator Design

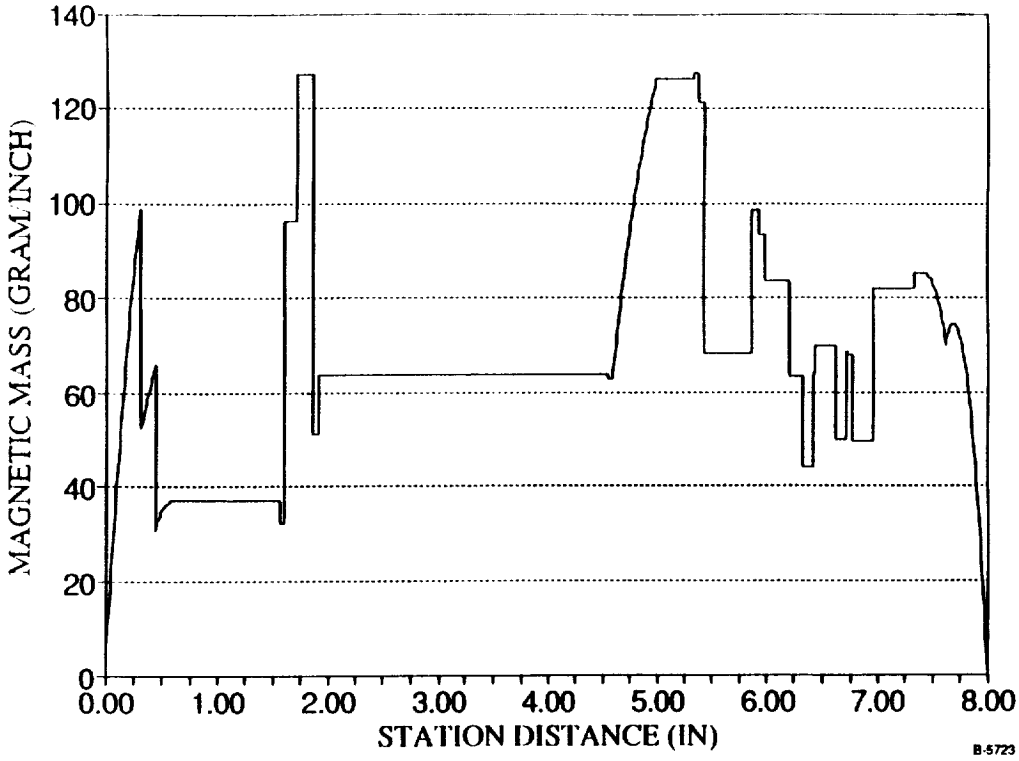

Figure 3. Magnetic Mass Distribution in the Small Scale Simulator

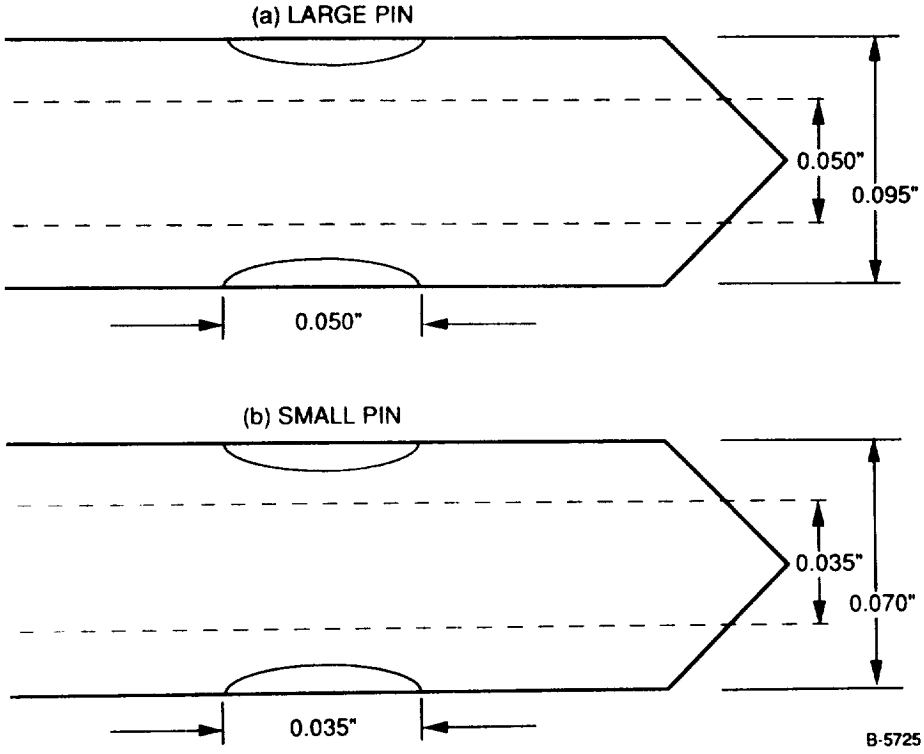

Figure 4. Large and Small Piercing Pin Design for Small Scale Simulator

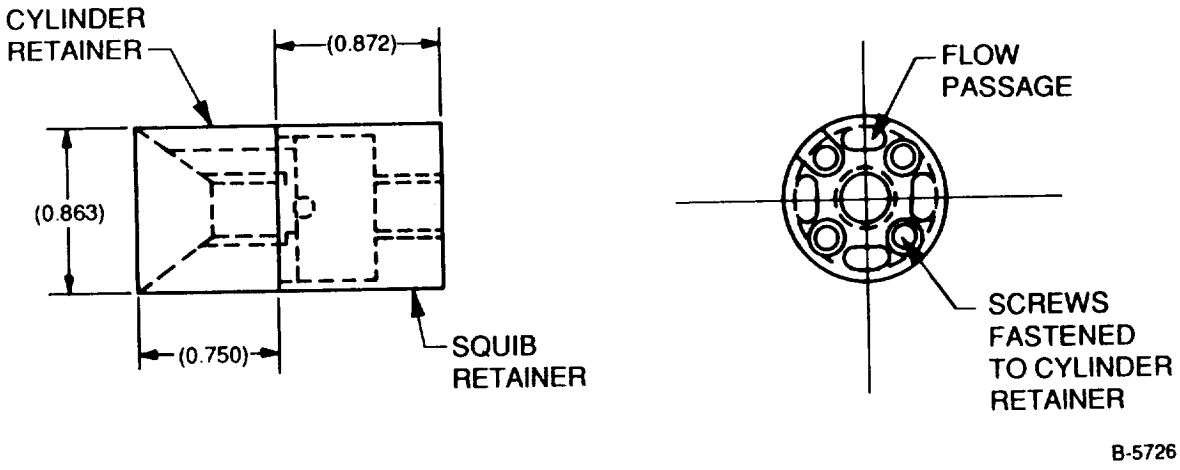

Figure 5. Cylinder and Squib Retainer Arrangement in Small Scale Simulator

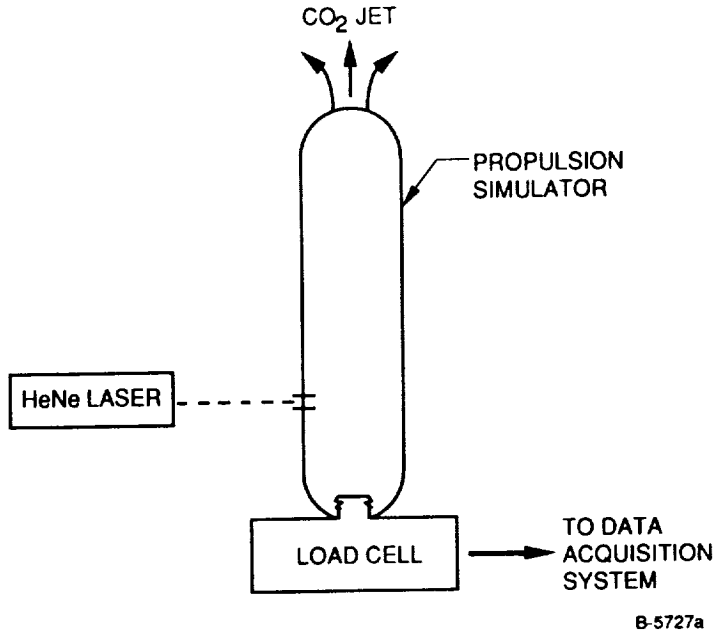

(a) Thrust Measurements

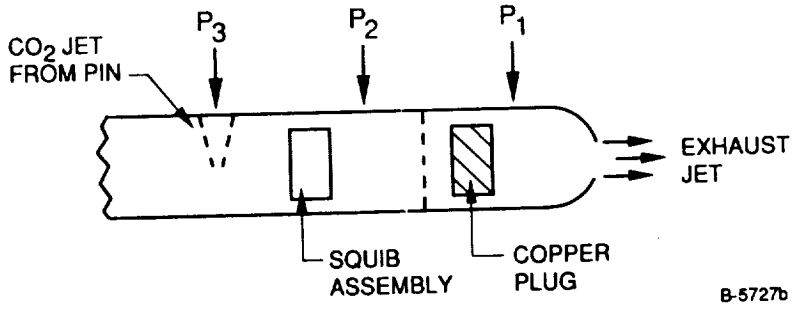

(b) Pressure Measurement

Figure 6. Schematic of Small-Scale Simulator Static Testing

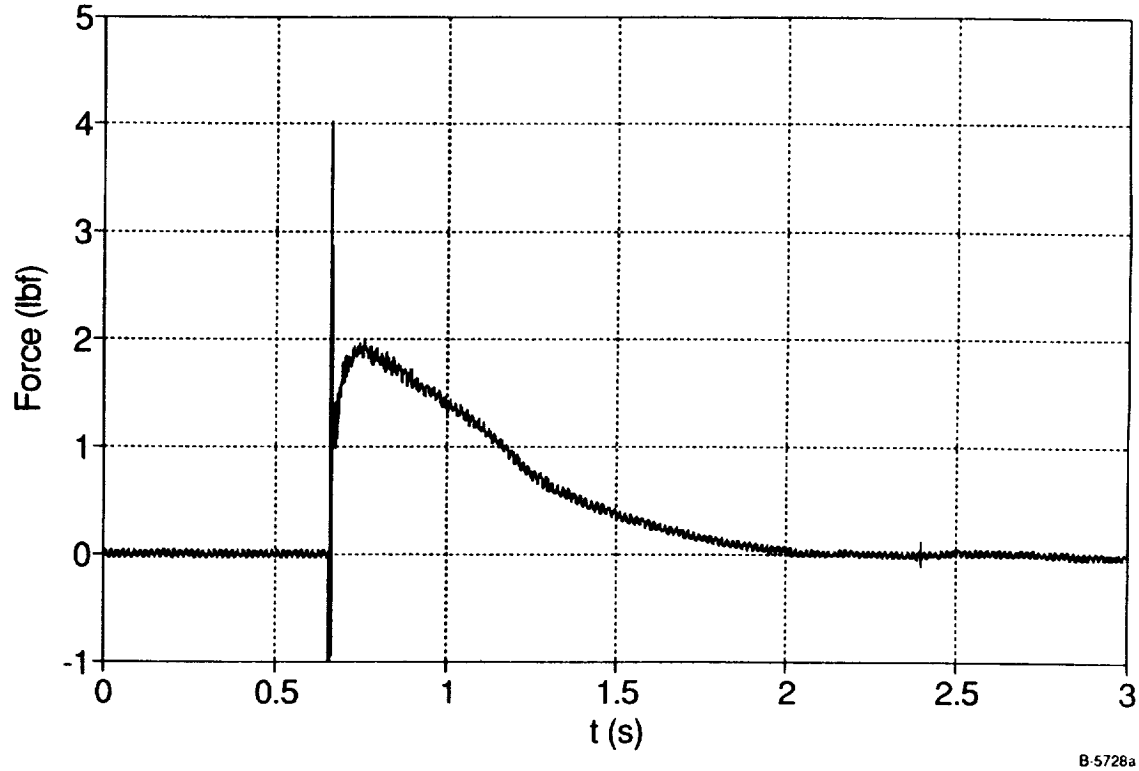

(a) Thrust versus Time

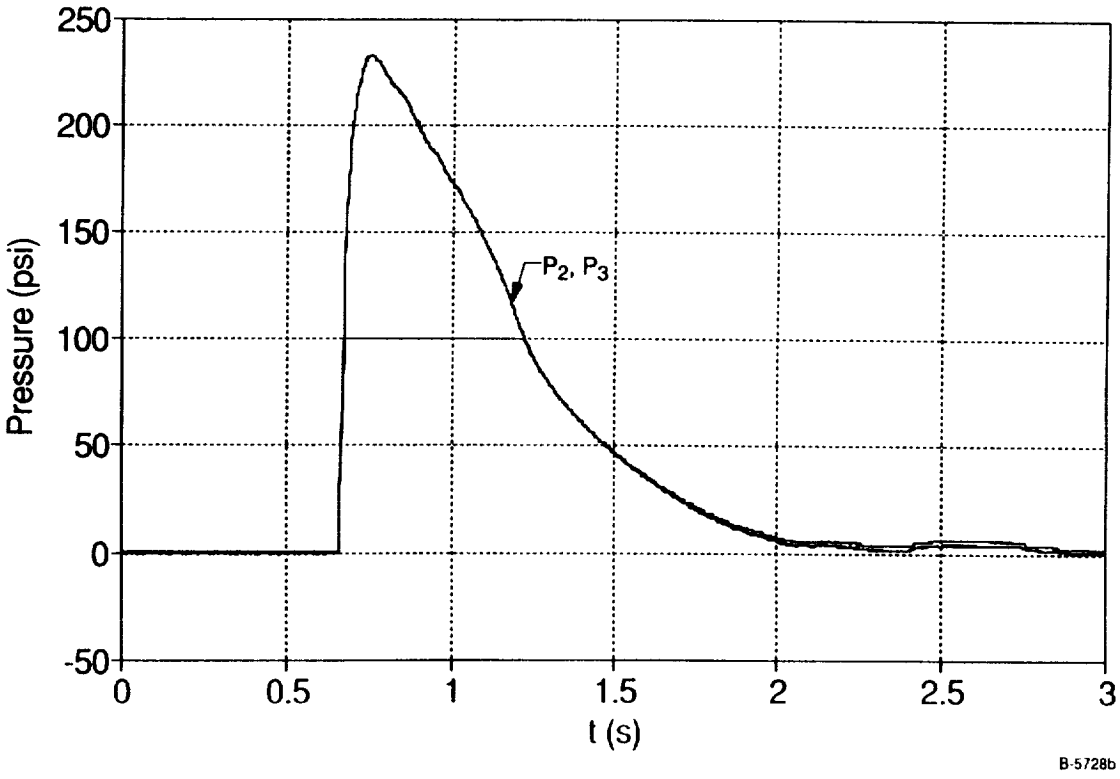

(b) Pressure versus Time

Figure 7. Thrust and Pressure Time History for Baseline Configuration Without Copper Plug (large pin, 0.098-in. diameter nozzle, vertical up orientation)

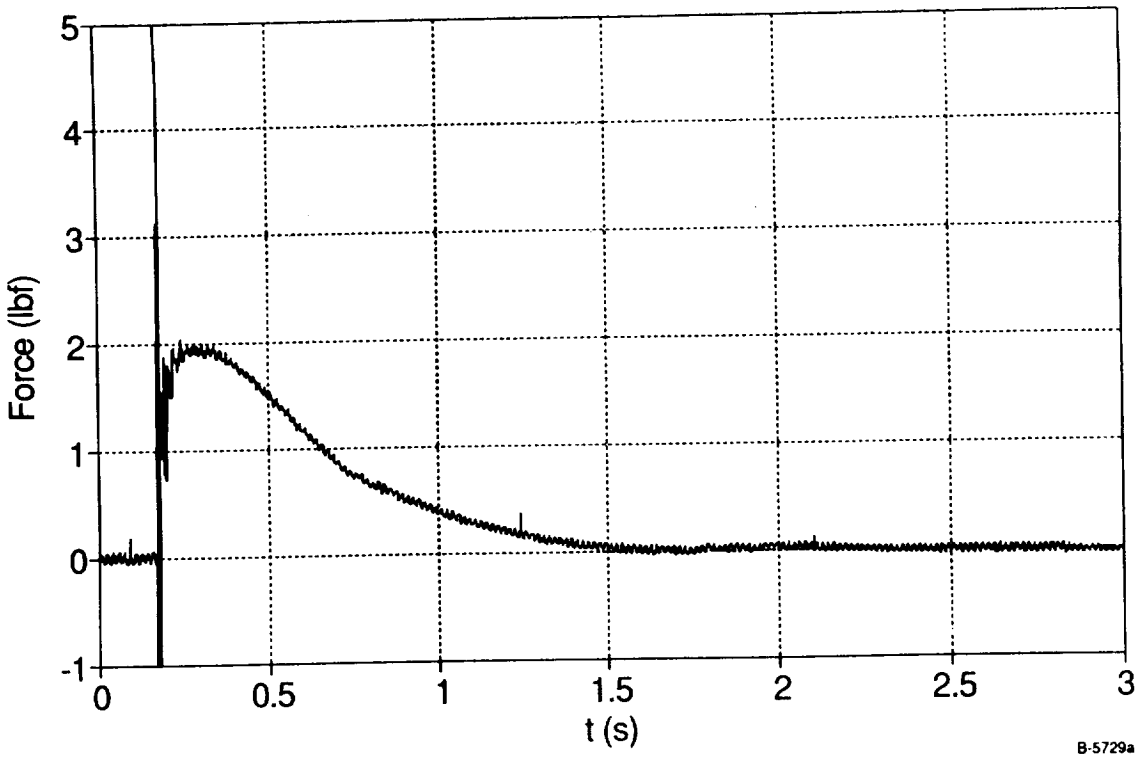

(a) Thrust versus Time

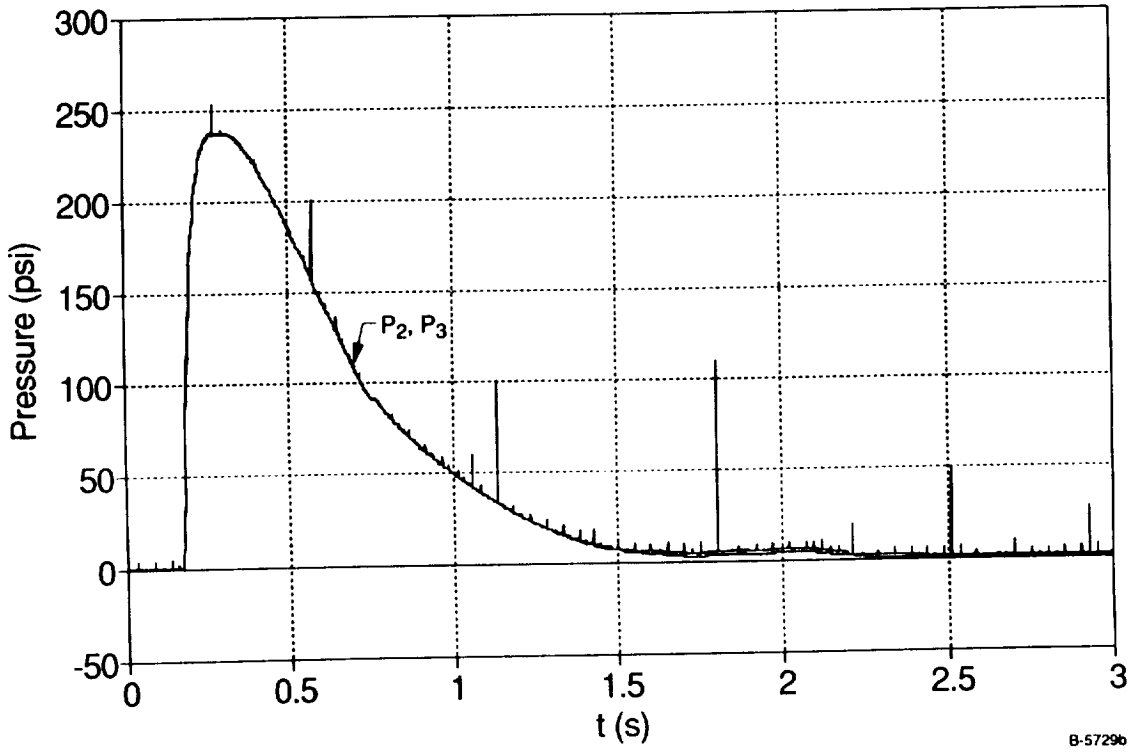

(b) Pressure versus Time

Figure 8. Effect of Three Sets of 2 mm Diameter Copper Spheres son Thrust and Pressure Time History (large pin, 0.098-in.diameter nozzle, vertical up simulator orientation)

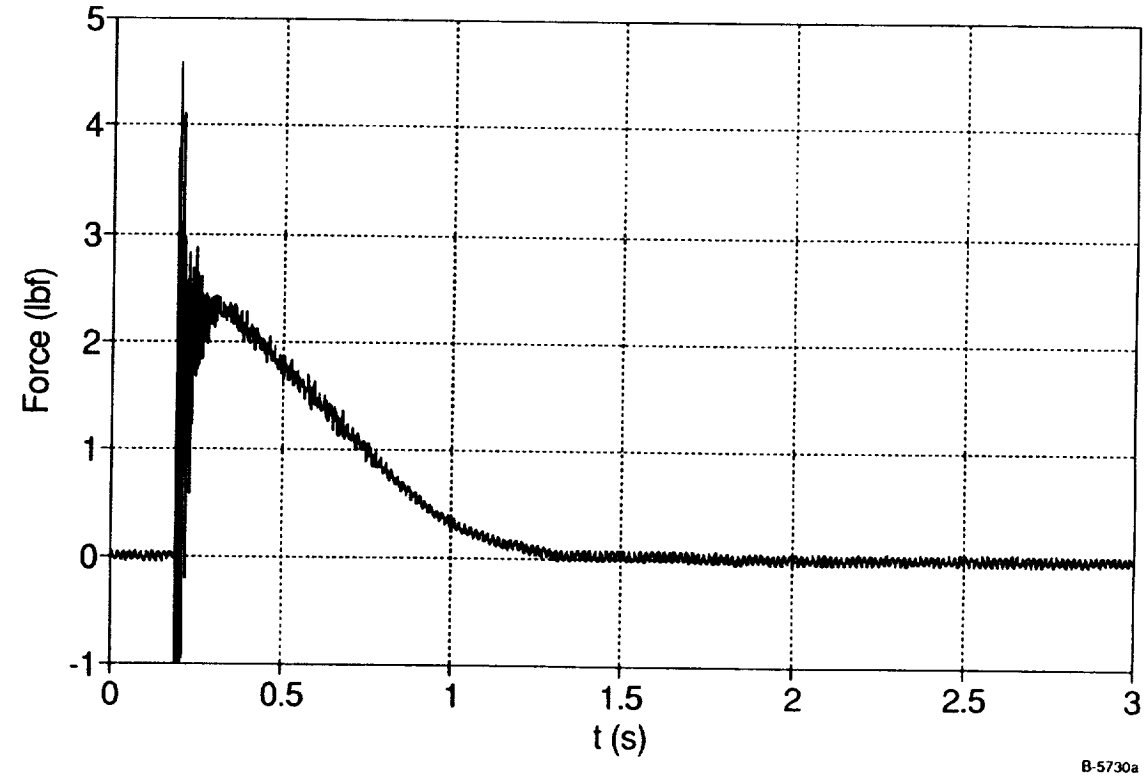

(a) Thrust versus Time

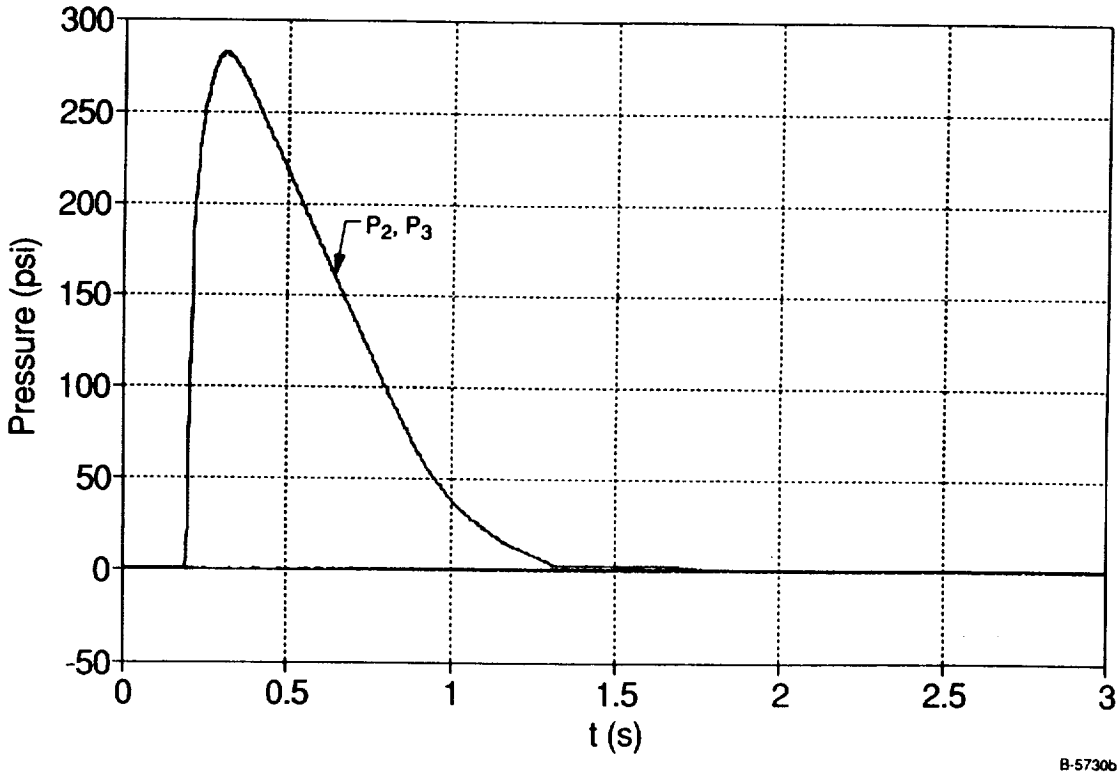

(b) Pressure versus Time

Figure 9. Effect of Horizontal Simulator Orientation on Thrust and Pressure Time History (large pin, 0.098-in.diameter nozzle, three sets of 2 mm copper spheres)

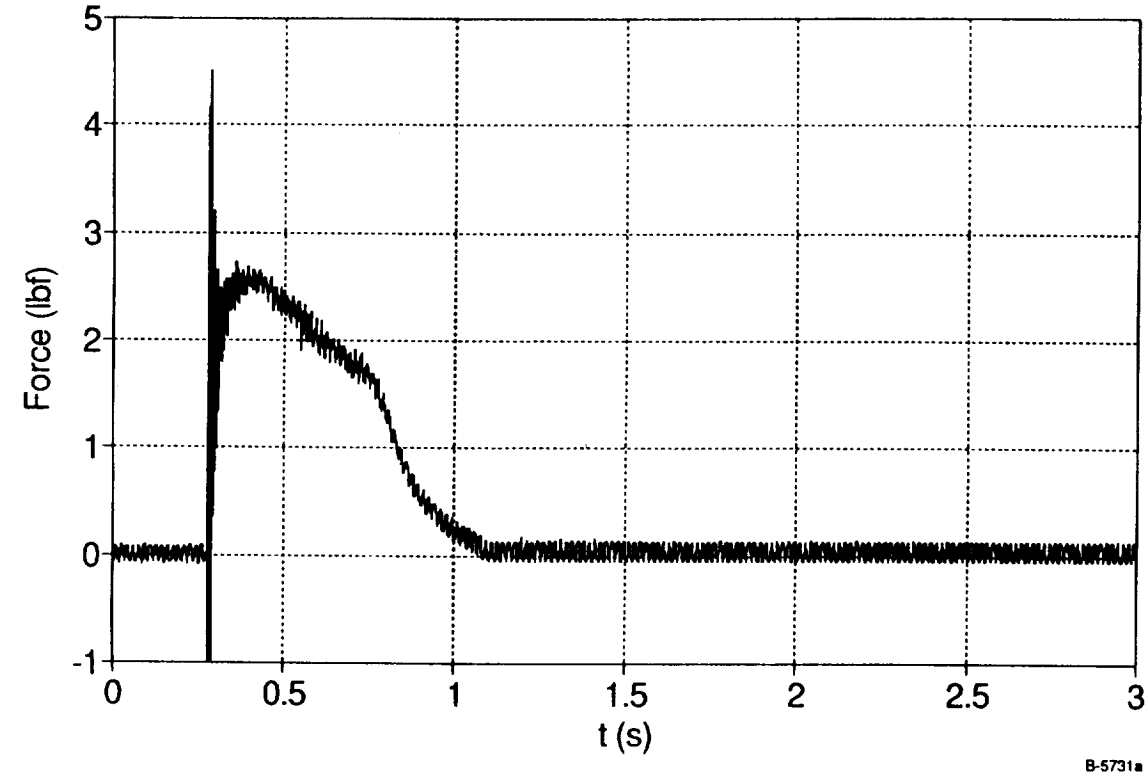

(a) Thrust versus Time

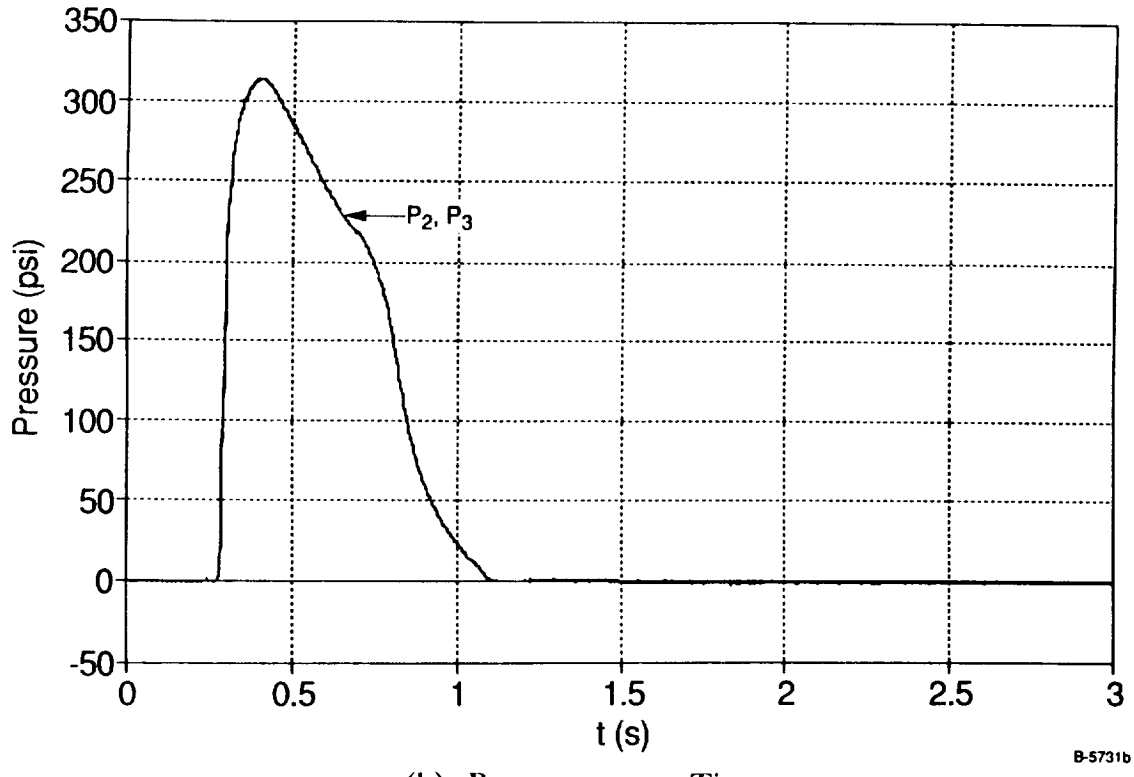

(b) Pressure versus Time

Figure 10. Effect of Vertical Down Simulator Orientation on Thrust and Pressure Time History (large pin, 0.098-in.diameter nozzle, three sets of 2 mm copper spheres)

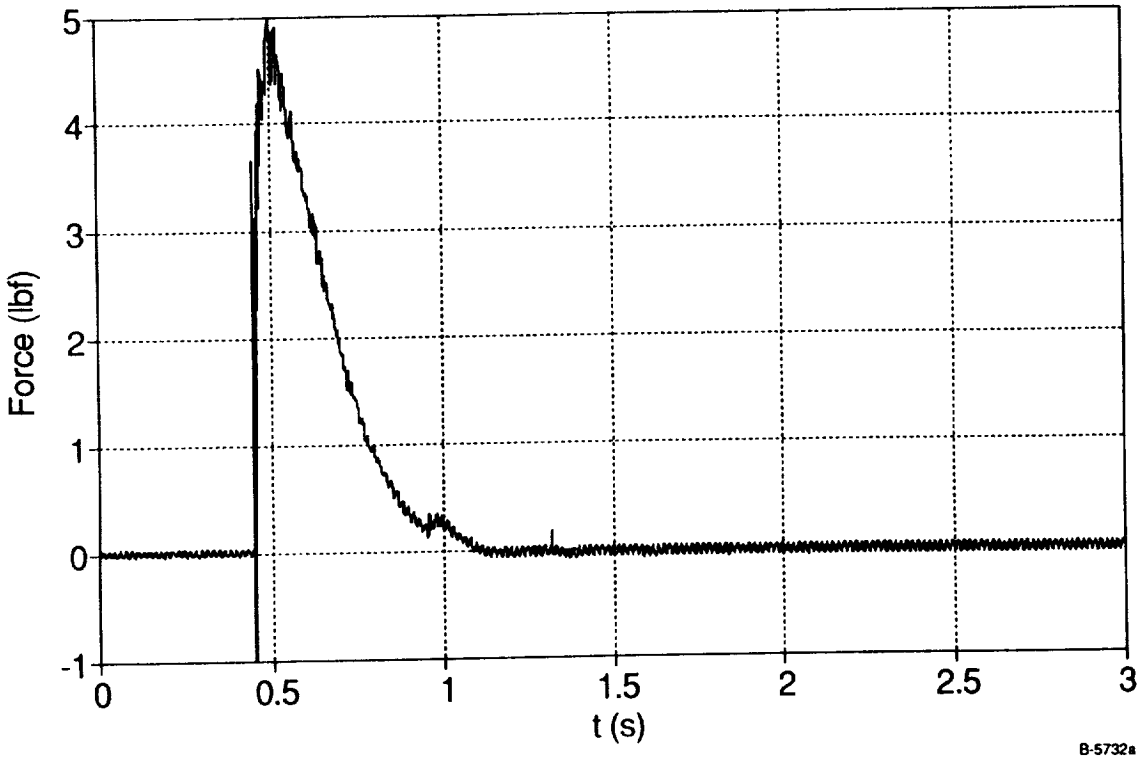

(a) Thrust versus Time

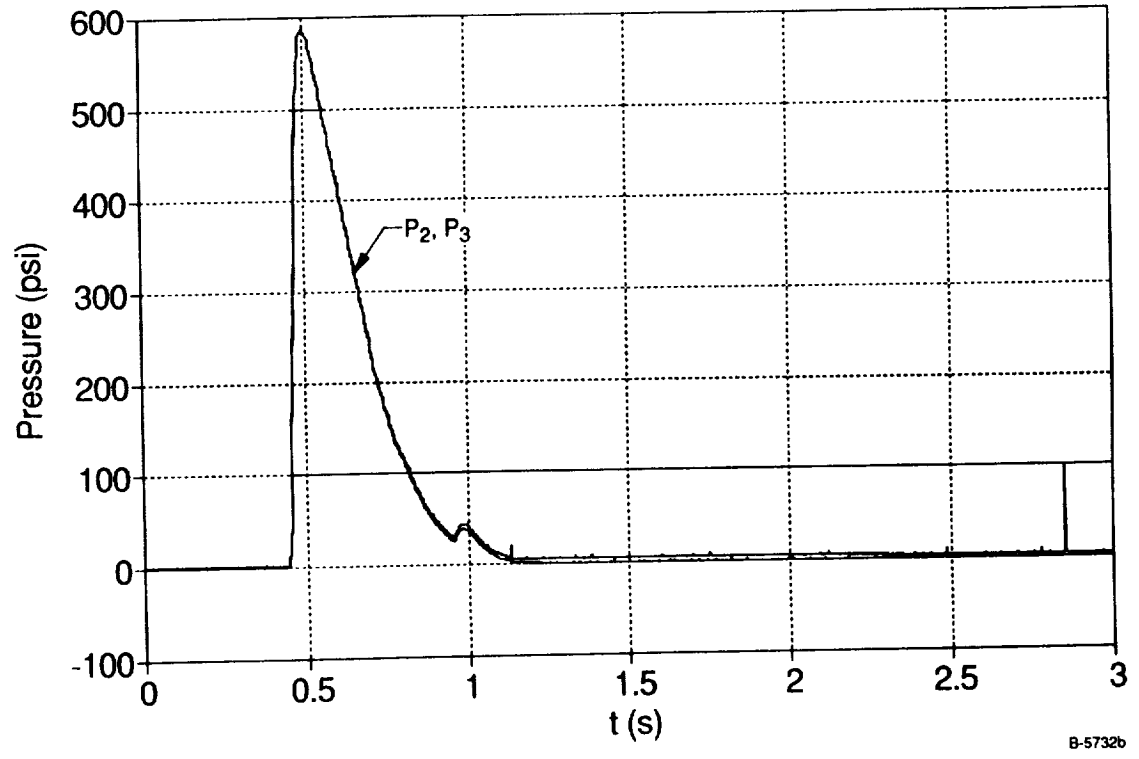

(b) Pressure versus Time

Figure 11. Effect of Increased CO_2 Mass Flow Rate on Thrust and Pressure Time History (large pin, 0.098-in.diameter nozzle, three sets of 2 mm copper spheres, vertical up simulator orientation)

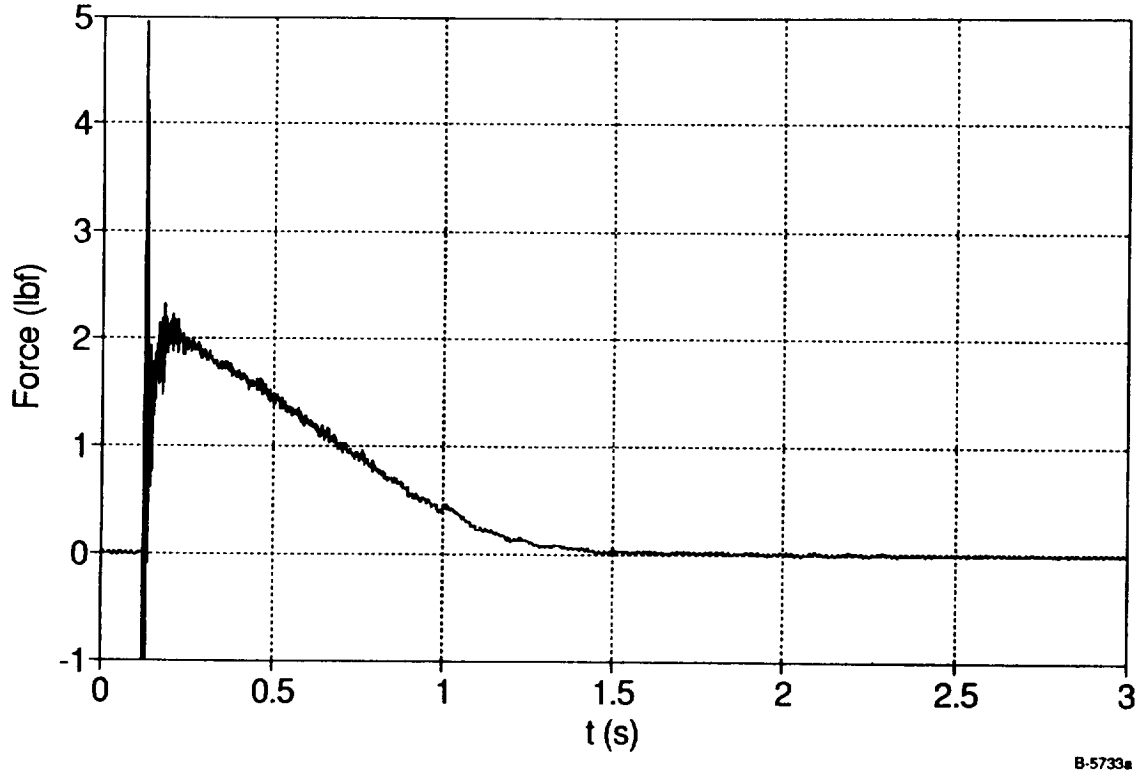

(a) Thrust versus Time

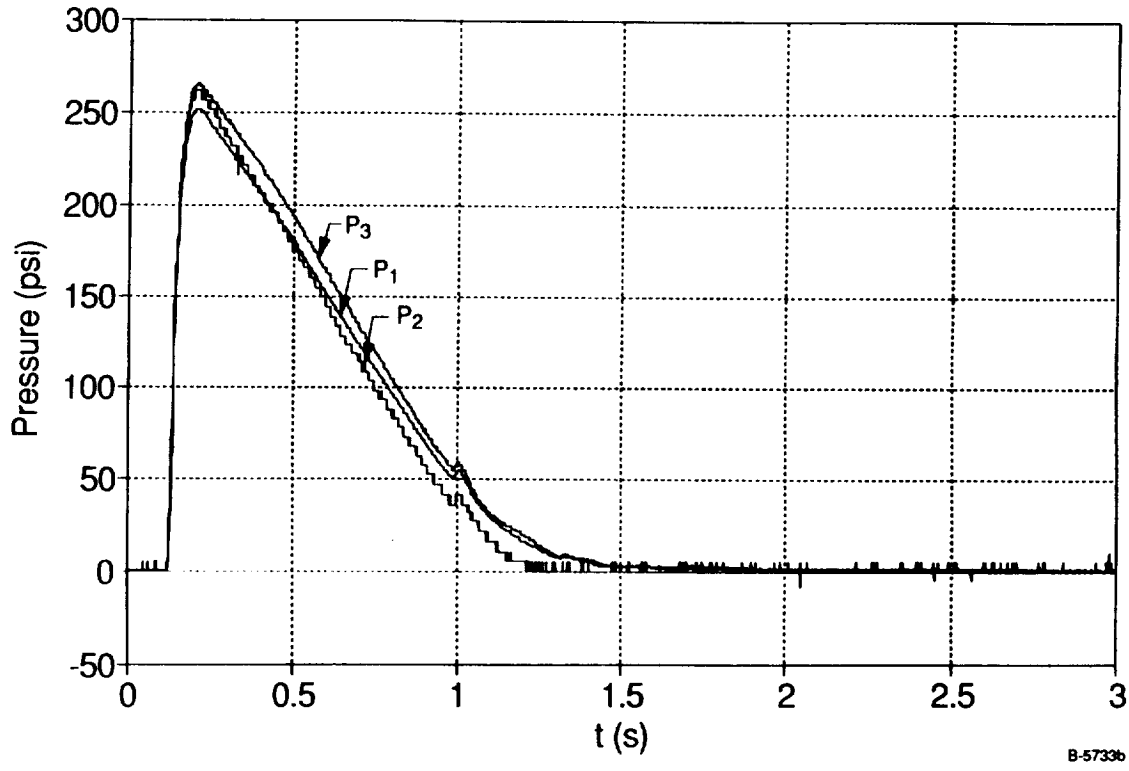

(b) Pressure versus Time

Figure 12. Effect of Copper Plug Structure on Thrust and Pressure Time History (large pin, 0.098-in.diameter nozzle, one set of 1 mm copper spheres, plus bronze wool, horizontal orientation)

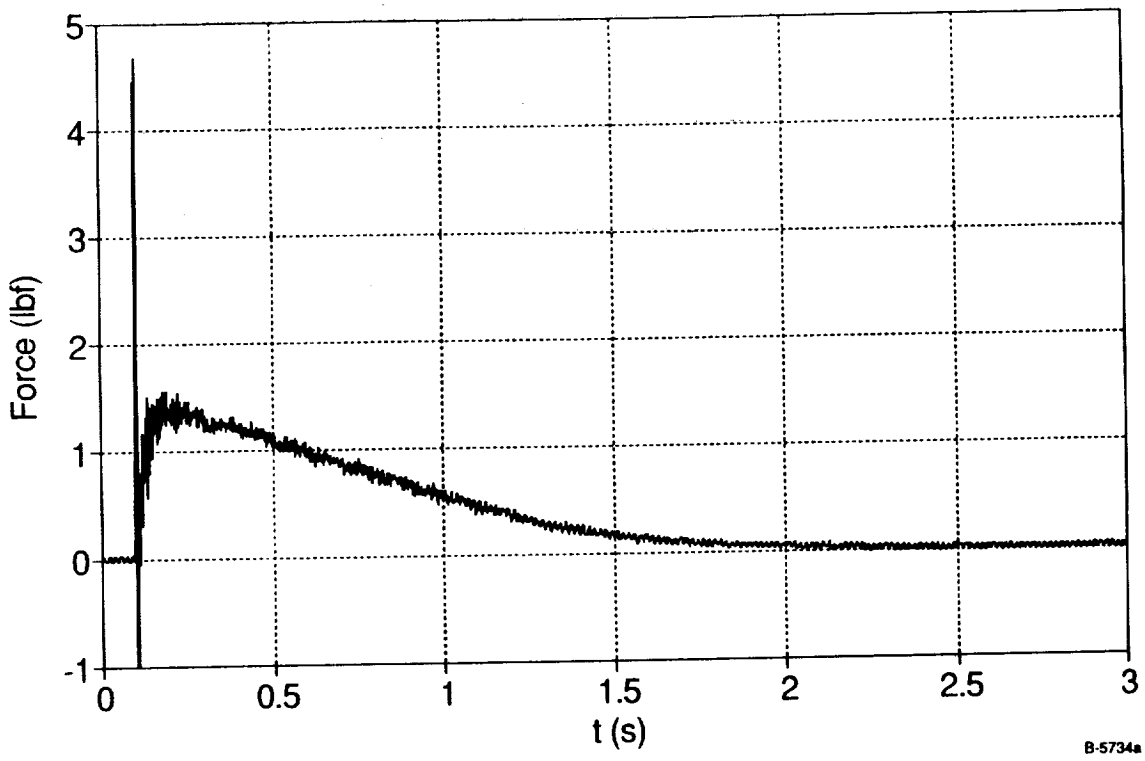

(a) Thrust versus Time

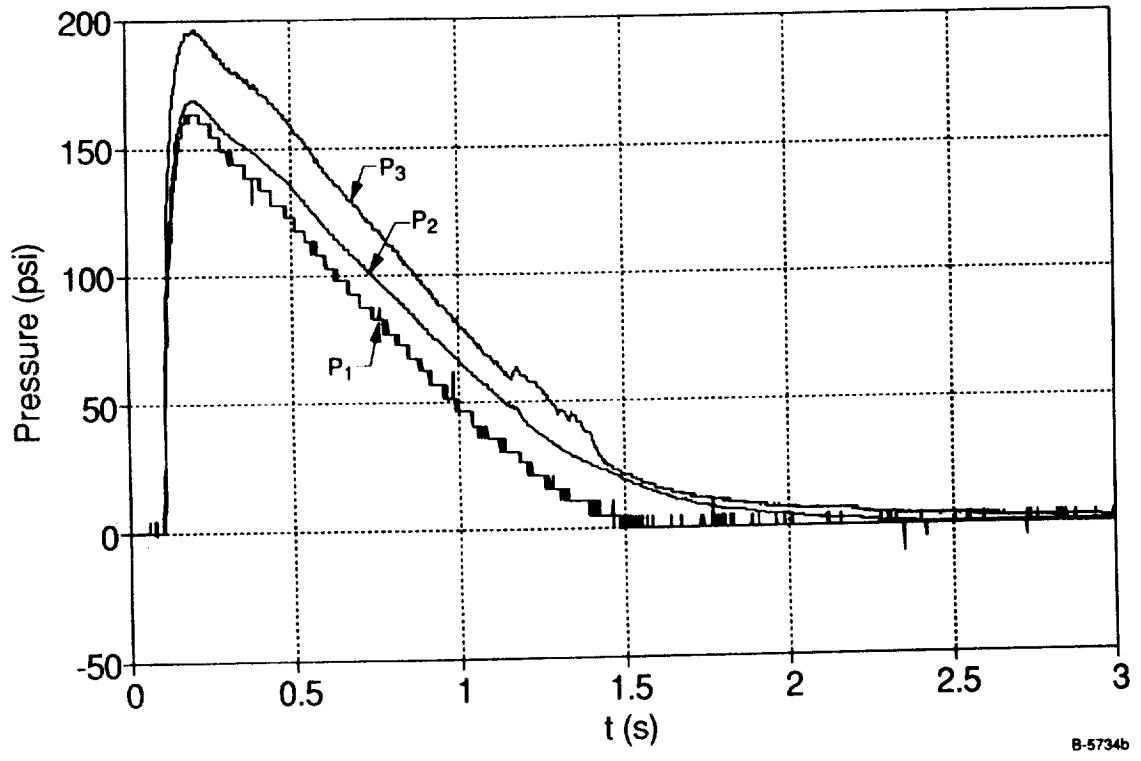

(b) Pressure versus Time

Figure 13. Effect of "Smaller" Pin on Thrust and Pressure Time History (0.098-in.diameter nozzle, one set of 1 mm copper spheres, plus bronze wool, horizontal orientation)

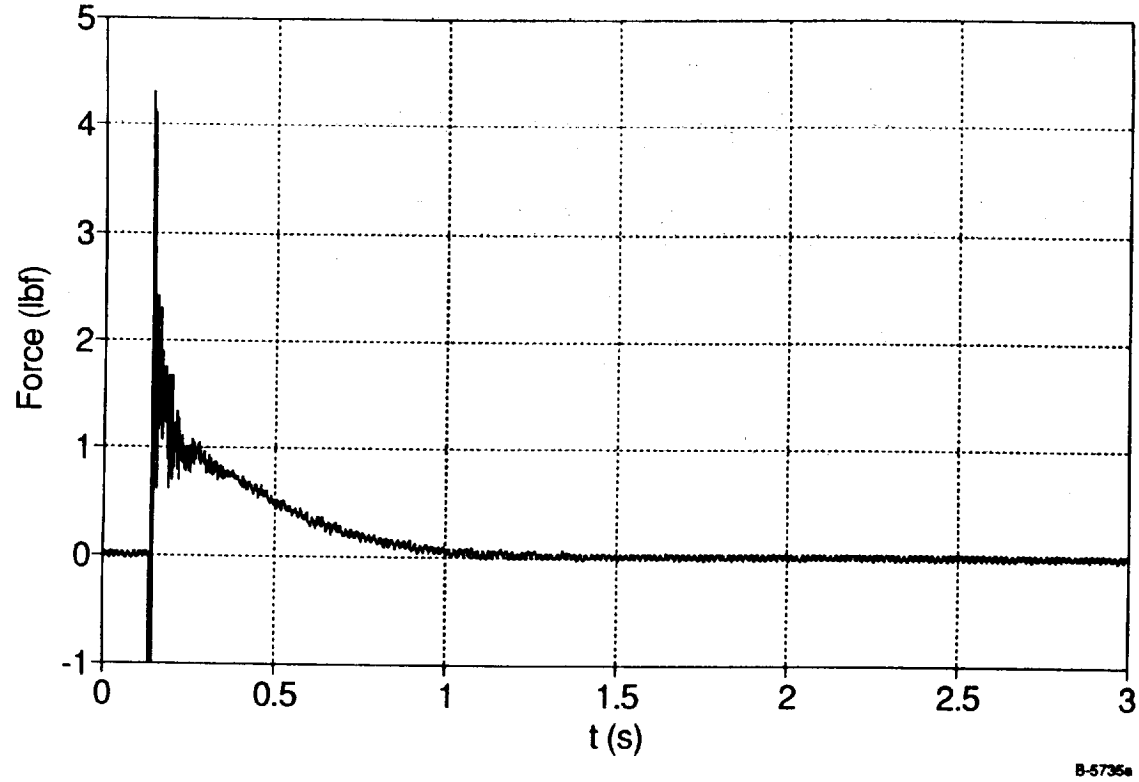

(a) Thrust versus Time

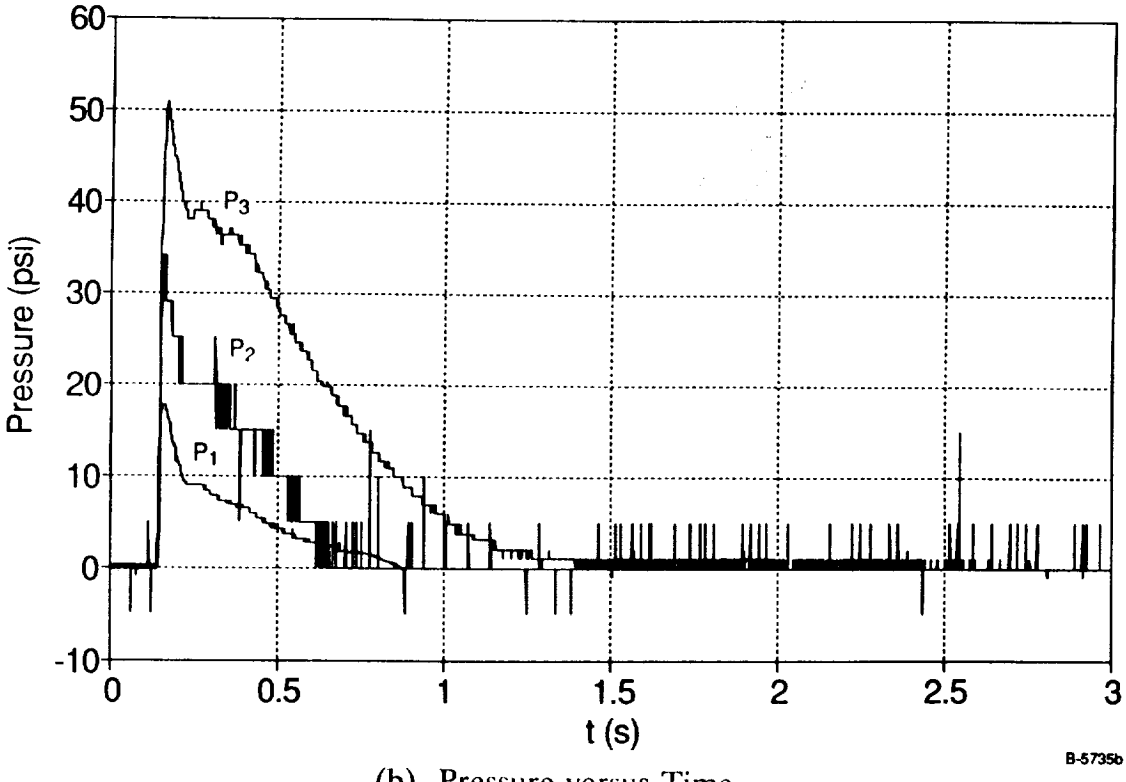

(b) Pressure versus Time

Figure 14. Effect of Exit Nozzle Diameter on Thrust and Pressure Time History (large pin, 0.295-in.diameter nozzle, one set of 1 mm copper spheres, plus bronze wool, horizontal orientation)

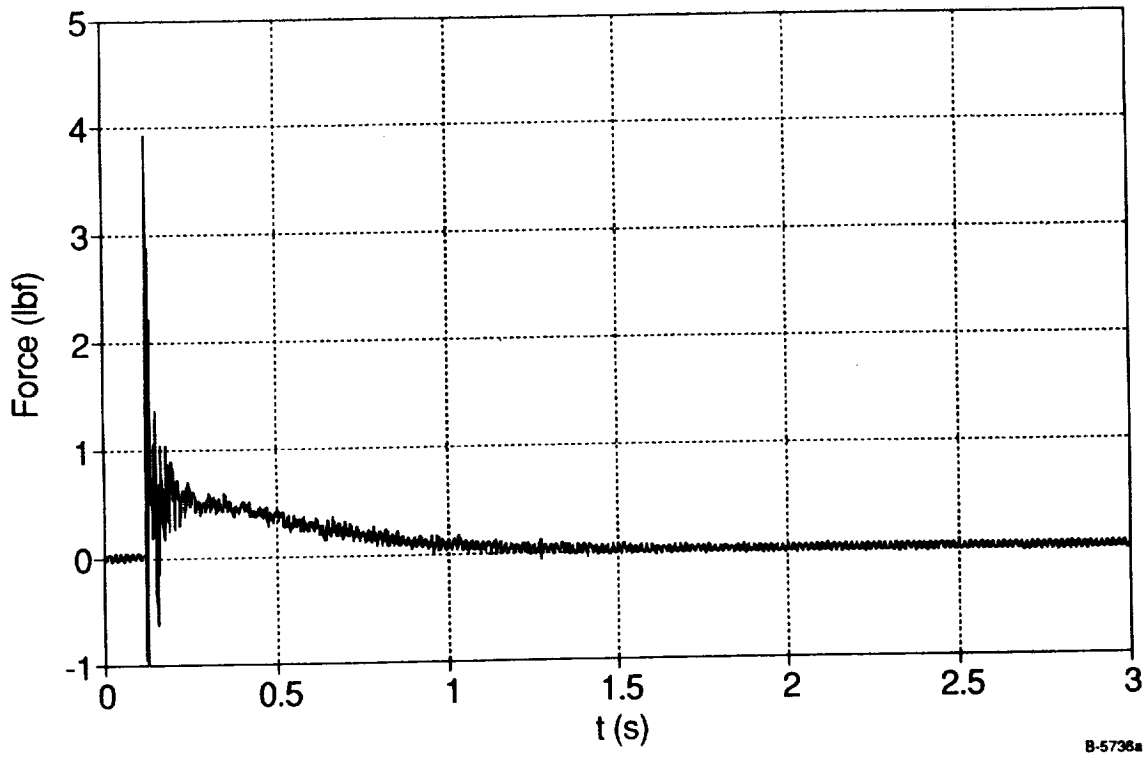

(a) Thrust versus Time

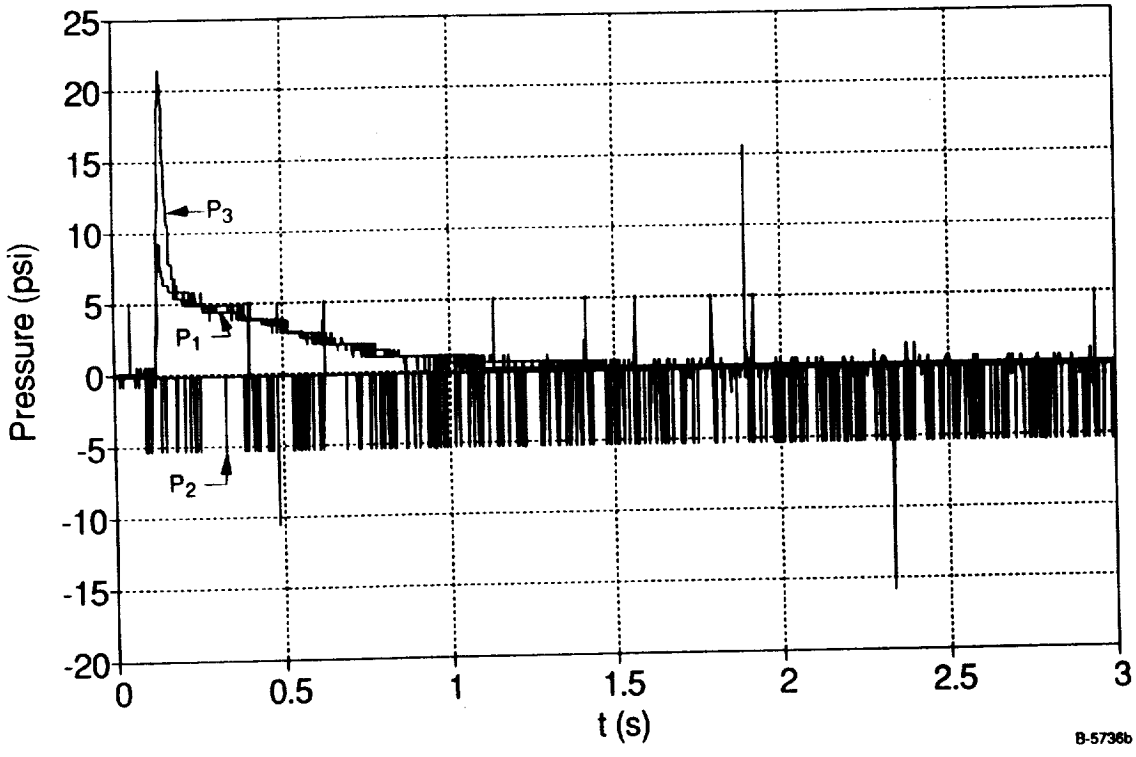

(b) Pressure versus Time

Figure 15. Effect of Removing Copper Plug on Thrust and Pressure Time History of Large Nozzle Diameter Simulator (0.295-in. nozzle diameter, horizontal orientation, large pin)

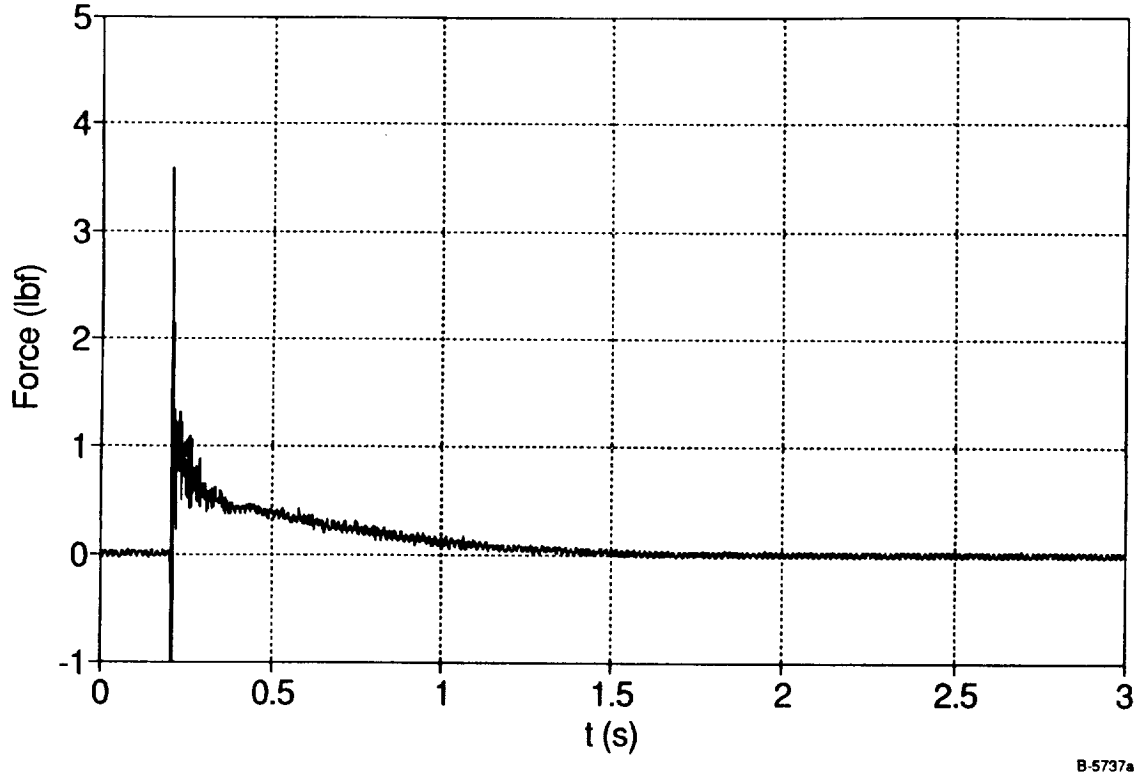

(a) Thrust versus Time

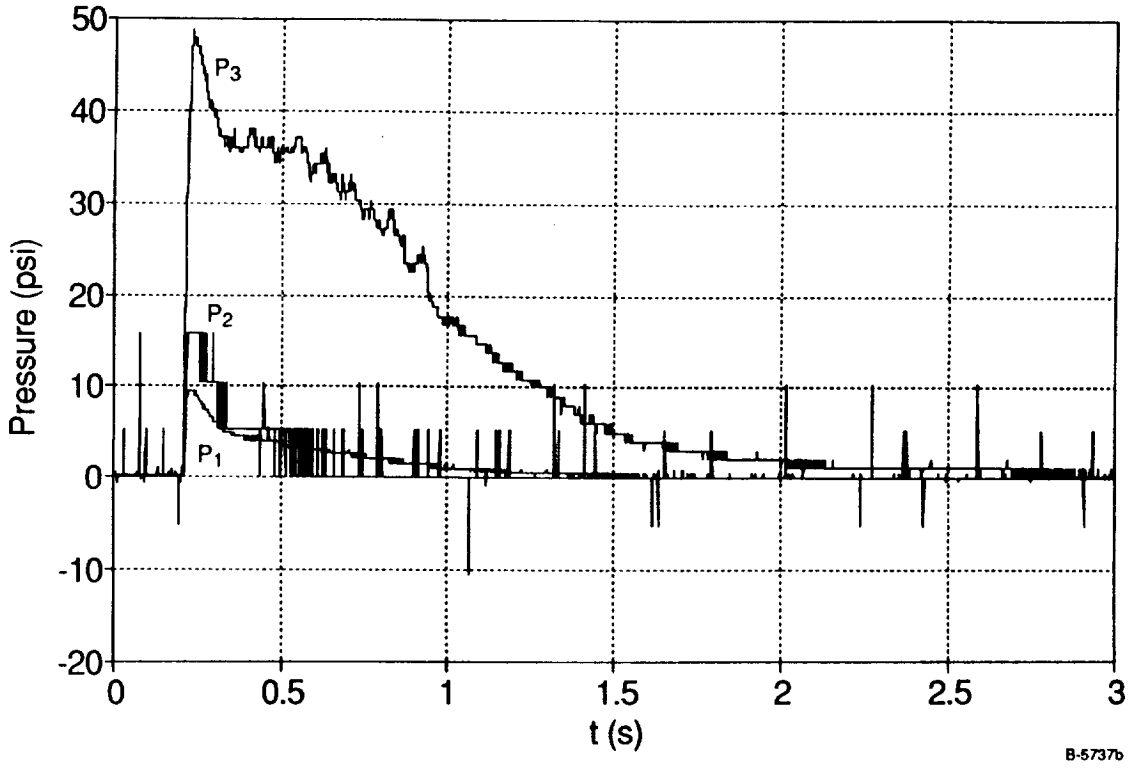

(b) Pressure versus Time

Figure 16. 0.295-in. Nozzle Diameter with "Small" Pin: Thrust and Pressure Time History (one set of 1 mm diameter copper spheres plus bronze wool, horizontal orientation)

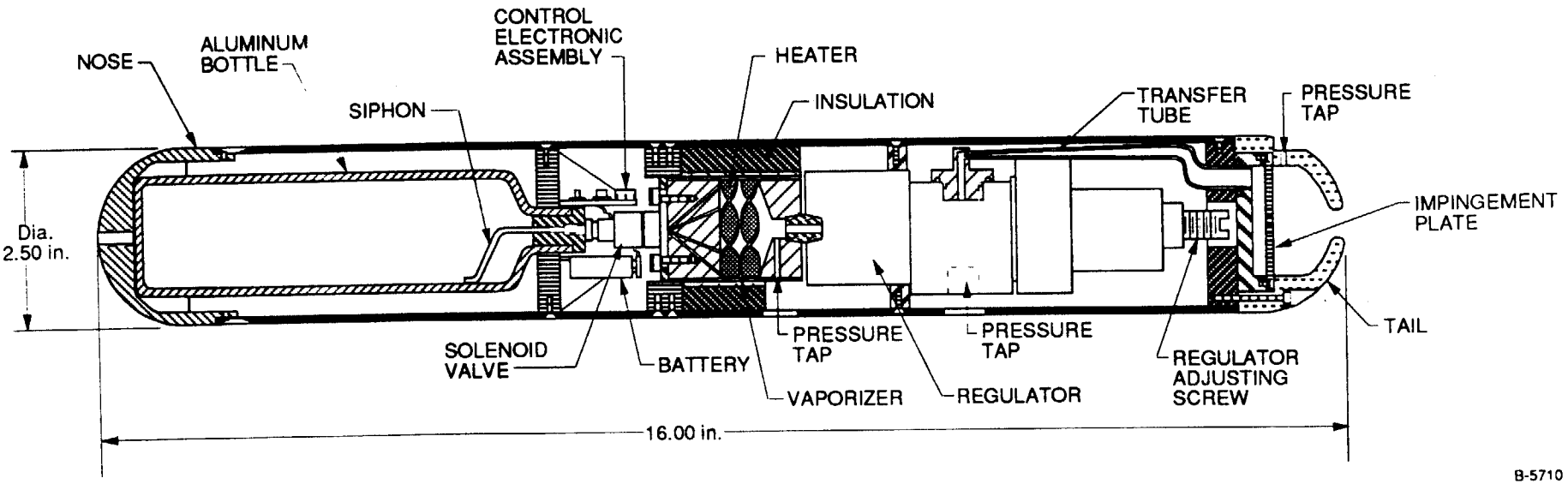

Figure 17. Preliminary Design of Large-Scale Propulsion Simulator